

Article

Comprehensive *In Silico* Analysis of the *NHX* (Na⁺/H⁺ Antiporter) Gene in Rice (*Oryza sativa* L.)

Hoa Hai Thi Bui¹, Duong Huy Nguyen^{2,*} , Le Thu Thi Dinh¹, Hang Thu Thi Trinh¹, Thoa Kim Vu¹ and Van Ngoc Bui^{2,3,*}

- ¹ Institute of Biological and Food Technology, Hanoi Open University, 101B Nguyen Hien Street, Hai Ba Trung District, Hanoi 10072, Vietnam; haihoacnsh@hou.edu.vn (H.H.T.B.); thulecnsh@hou.edu.vn (L.T.T.D.); trinhhangcnsh@hou.edu.vn (H.T.T.T.); kimthoacnsh@hou.edu.vn (T.K.V.)
- ² Institute of Biotechnology, Vietnam Academy of Science and Technology, 18 Hoang Quoc Viet Road, Cau Giay District, Hanoi 10072, Vietnam
- ³ School of Biotechnology, Graduate University of Science and Technology, Vietnam Academy of Science and Technology, 18 Hoang Quoc Viet Road, Cau Giay District, Hanoi 10072, Vietnam
- * Correspondence: nguyenhuyduongts@gmail.com (D.H.N.); bui@ibt.ac.vn (V.N.B.)

Abstract: The Na⁺/H⁺ antiporter (*NHX*) gene family plays a pivotal role in plant salt tolerance in regulating intracellular Na⁺ and H⁺ homeostasis. In this study, seven candidate *OsNHX* genes (*OsNHX1* to *OsNHX7*) were identified in the rice genome and classified into three phylogenetic clusters (Vac, Endo, and PM) based on their predicted subcellular localization. Five *OsNHX* gene pairs (*OsNHX1/OsNHX2*, *OsNHX1/OsNHX3*, *OsNHX1/OsNHX4*, *OsNHX2/OsNHX6*, and *OsNHX5/OsNHX6*) were found to have arisen from dispersed duplication events and exhibited purifying selection, indicating functional conservation. Analysis of *cis*-regulatory elements (CREs) revealed a diverse range of elements associated with tissue-specific expression, hormone signaling, and stress responses, particularly to dehydration and salinity. Notably, CREs associated with tissue/organelle-specific expression and stress responses were the most abundant, suggesting a potential role for *OsNHX* genes in regulating growth, development, and stress tolerance in rice. Importantly, expression profiling revealed that *OsNHX1*, *OsNHX2*, *OsNHX3*, and *OsNHX5* were upregulated under salt stress, with significantly higher expression levels in the salt-tolerant rice cultivar Pokkali compared to the salt-sensitive cultivar IR64. Our findings provide a comprehensive analysis of the evolutionary, structural, and functional features of the *OsNHX* gene family and highlights their critical role in rice salt tolerance, offering insights into potential applications for crop improvement.

Keywords: conserved motifs; evolutionary relationship; *NHX* gene family; rice; salt stress



Academic Editor: Mohammad Anwar Hossain

Received: 3 December 2024

Revised: 28 December 2024

Accepted: 3 January 2025

Published: 6 January 2025

Citation: Bui, H.H.T.; Nguyen, D.H.; Dinh, L.T.T.; Trinh, H.T.T.; Vu, T.K.; Bui, V.N. Comprehensive *In Silico* Analysis of the *NHX* (Na⁺/H⁺ Antiporter) Gene in Rice (*Oryza sativa* L.). *Int. J. Plant Biol.* **2025**, *16*, 6. <https://doi.org/10.3390/ijpb16010006>

Copyright: © 2025 by the authors. Licensee MDPI, Basel, Switzerland. This article is an open access article distributed under the terms and conditions of the Creative Commons Attribution (CC BY) license (<https://creativecommons.org/licenses/by/4.0/>).

1. Introduction

Salinity stress, characterized by excessive accumulation of Na⁺ ions within plant cells, disrupts essential physiological processes and impairs plant growth and development [1,2]. These adverse effects are primarily due to the induction of ion toxicity [3], the inhibition of water absorption [4], nutritional imbalance [5], and oxidative stress [6], ultimately leading to a significant decrease in the overall crop productivity [2,7]. Therefore, understanding the mechanisms of salinity tolerance, particularly the roles of genes such as Na⁺/H⁺ exchangers (*NHX*), high-affinity potassium transporters (*HKT*), and salt overly sensitive (*SOS*) transporters, is crucial for developing strategies to improve crop yield in saline environments.

Plants cope with salinity stress through various physiological, biochemical, and molecular mechanisms. These include the regulation of growth and development, ion homeostasis, osmotic regulation, ion transport, detoxification, and the accumulation of compatible solutes [8,9]. Among these adaptive mechanisms, maintaining cellular ion and pH homeostasis is a critical strategy for plant survival and growth under salt stress [10].

$\text{Na}^+/\text{H}^+/\text{K}^+$ transporters, which are members of the integral membrane protein family, are well-established for their pivotal role in maintaining ion homeostasis under saline conditions. They regulate the influx and efflux of Na^+ , H^+ , and K^+ ions, retain K^+ in the cytosol, and sequester toxic ions, such as Na^+ into the vacuole [8,11]. These proteins primarily belong to families such as HKT, NHX, and SOS transporters. Many studies have demonstrated the role of these transporters in ion transport, sequestration, and compartmentation into cells and organelles, enabling plants to adapt to salinity stress [12–14]. While some HKT transporters were found to mediate Na^+-K^+ cotransport into root cells [15,16], both NHX and SOS transporters act as antiporters, exchanging $\text{Na}^+/\text{H}^+/\text{Li}^+$ ions across the vacuole, Golgi apparatus, or plasma membrane [17,18].

Na^+/H^+ exchangers are also known as NHXs in plants, NHEs in animals, or NHAs in the yeast *S. cerevisiae* [11]. In plants, all Na^+/H^+ exchangers belong to the CPA1 protein subfamily, which is conserved in most organisms, from algae to flowering plants [19,20]. Based on protein sequence similarity and subcellular localization, members of the CPA1 family are divided into two primary clades: NHX/NHE and NhaP/SOS, located in intracellular (IC) and plasma membrane (PM) compartments, respectively [19,21]. The NhaP/SOS clade, derived from the prokaryotic NhaP protein, encompasses NHX antiporters responsible for Na^+/H^+ exchange across the plasma membrane [19,22]. In contrast, all identified plant NHX proteins belong to the intracellular (IC) group, further divided into class I (tonoplasts, such as vacuolar) and class II (endosomal compartments like the trans-Golgi network) [23,24]. Previous studies have shown that the NHX protein family typically consists of 10 to 12 membrane helices (TMs), in which the amiloride binding site (FFIYLLPPI) located at TM3 of the N-terminus is a characteristic feature of Vac-class NHX proteins [25,26]. In general, Na^+/H^+ antiporters contain the Na^+/H^+ exchanger domain (PF00999) found in the Pfam database [27].

In the model plant *Arabidopsis thaliana*, the Na^+/H^+ antiporters comprise eight members, which are divided into three subgroups based on their location, revealing their diverse functions in salt tolerance, pH regulation, and cellular development [11,25]. Specifically, AtNHX1-4 is referred to as the vacuolar NHXs class, primarily sequestering excess Na^+ into the vacuole [28]; AtNHX5 and AtNHX6 are located in the endosomal compartments [23]; and AtNHX7-8 proteins are found in the plasma membrane [29]. The *Arabidopsis* NhaP protein, also known as AtSOS1 (sometimes referred to as AtNHX7), is responsible for Na^+/H^+ exchange across the plasma membrane, while its homolog, AtNHX8, only conducts Li^+/H^+ exchange [22]. Although the NHX gene family has been extensively studied in *Arabidopsis*, rice may have evolved distinct structures, levels of conservation and functions for these genes. Furthermore, the expression patterns of *OsNHX* genes and their associated CREs may differ between rice and *Arabidopsis* under various environmental conditions. Therefore, a comparative analysis of *OsNHX* genes with their *Arabidopsis* counterparts could reveal important differences in their functions and regulatory mechanisms.

Previous studies have demonstrated the role of NHX genes in enhancing salt tolerance in rice. For instance, Fukuda et al. (2011) reported that salt stress, hyperosmotic stress, and ABA stress induce the expression of *OsNHX1*, *OsNHX2*, *OsNHX3*, and *OsNHX5* in rice, highlighting the potential role of these genes in salt tolerance [30]. Another study showed that introducing the *OsNHX1* gene into perennial ryegrass enabled the plant to withstand high salt concentrations (350 mM) for 10 weeks [31]. Similarly, in a study by

Han et al. (2014), transgenic tobacco plants overexpressing the wheat *TaNHX3* gene exhibited enhanced salt tolerance as a result of improved physiological processes [32]. Furthermore, the overexpression of the *AtNHX1* gene from *Arabidopsis thaliana* in tomatoes and the *SsNHX1* gene from *Salsola collina* in *Medicago sativa* L. significantly improved salt tolerance in these plants [33,34]. These studies collectively demonstrate the role of *NHX* genes in enhancing salt tolerance, not only in rice but also in other plant species.

Although Na^+/H^+ antiporters in rice have been cloned and functionally characterized, demonstrating their effectiveness in regulating intracellular Na^+/K^+ balance [35] and improving salt tolerance [30,36], a comprehensive and systematic investigation of these antiporters has not yet been fully conducted. In this study, we identified Na^+/H^+ antiporters from the genome of *Oryza sativa* L. using a comprehensive *in silico* approach and the well-characterized *AtNHX1–8* proteins as references. Additionally, several features of *OsNHX* genes were analyzed, including gene structure, conserved protein domains, synteny analysis, phylogenetic relationships, analysis of *cis*-regulatory elements, and *OsNHX* gene expression profiles. By integrating genomic, phylogenetic, and comparative analyses, this study aims to elucidate the contribution of Na^+/H^+ antiporters to salinity stress adaptation as well as provide significant insights into the functional diversity and conserved characteristics of Na^+/H^+ antiporters in rice.

2. Materials and Methods

2.1. Identification and Characterization of *NHX* Genes in the Rice Genome

The rice *NHX* genome and *Arabidopsis thaliana* (*AtNHXs*) gene sequences were retrieved from the Phytozome V13 database (<https://phytozome-next.jgi.doe.gov/>, accessed on 13 May 2024) [37]. To identify Na^+/H^+ transporter genes in rice (*Oryza sativa* L.), we utilized the following approaches: Firstly, we used query sequences (PF00999) to screen all Na^+/H^+ antiporter protein sequences from the rice genome in the Phytozome V13 database. Secondly, putative Na^+/H^+ antiporter protein sequences were further identified by aligning them with the *AtNHXs* (*AtNHX1* to *AtNHX8*) sequences (E-value cut-off of 1.0×10^{-10}) to eliminate the cation/ H^+ exchanger (CHX) and the K^+ efflux antiporter (KEA). Next, to reduce redundancy, candidate genes with more than 90% sequence identity were excluded. Finally, the Hidden Markov model (HMM) (<https://www.ebi.ac.uk/Tools/hmmer/search/phmmer>, accessed on 13 May 2024) with default parameters [38], SMART (<http://smart.embl-heidelberg.de/>, accessed on 13 May 2024) [39], and Batch CD-Search (<https://www.ncbi.nlm.nih.gov/cdd>, accessed on 13 May 2024) [40] tools were employed to verify the presence of the conserved Na^+/H^+ exchanger domain in the *NHX* protein structure. Candidate proteins possessing at least one such domain were definitively classified as Na^+/H^+ antiporters in *Oryza sativa*.

The ExPASy website (<https://web.expasy.org/protparam/>, accessed on 14 May 2024) was used to predict and calculate the physical and chemical properties of Na^+/H^+ proteins, such as the isoelectric point (pI) and the molecular weight (MW). The number of transmembrane domains (TM) and the signal peptide of *NHX* proteins were predicted using the Phobius online tool (<https://phobius.sbc.su.se/index.html>, accessed on 14 May 2024) [41]. The online tool NetPhos 3.1 (<https://services.healthtech.dtu.dk/services/NetPhos-3.1/>, accessed on 14 May 2024) was used to predict phosphorylation sites of amino acids in *OsNHX* proteins [42].

2.2. Phylogenetic Analysis of *NHX* Family Proteins in Several Species

To investigate the phylogenetic relationships among *NHX* genes, we used *OsNHX* protein sequences from the Phytozome V13 database and six other plant species, including *Arabidopsis thaliana*, *Solanum lycopersicum*, *Cucurbita maxima*, *Lonicera japonica*, *Populus*

trichocarpa, and *Sorghum bicolor*, which were obtained from published articles [43–45]. The amino acid sequences of the NHX protein of rice and six selected species were used for multiple sequence alignment with the MUSCLE algorithm, and then a phylogenetic tree was constructed using the neighbor-joining (NJ) method with MEGA version 11 software with the bootstrap value of 1000 replicates [46]. The rice *NHX* genes were classified into subgroups (e.g., Vac, Endo, PM) based on their evolutionary relationships and predicted subcellular locations.

2.3. Gene Structures and Conservative Domains, and Cis-Regulatory Element Analysis

The gene structure (exon/intron organization) was analyzed using the nwk file of the phylogenetic tree of *OsNHX* genes and genomic DNA and coding sequences in the online tool Gene Structure Display Server (GSDS) 2.0 (<http://gsds.gao-lab.org/>, accessed on 14 May 2024) [47].

To further analyze the conserved domains of the *OsNHX* protein family members in *Oryza sativa*, the MEME suite online program (MEME version 5.57, <http://meme-suite.org/tools/meme>, accessed on 14 May 2024) was used for motif analysis, with a base width of 6–50 aa and a maximum number of 10 motifs [48].

For *cis*-regulatory elements, the 1500 nucleotide sequences upstream of *OsNHX* genes were extracted from the Phytozome V13 database and then analyzed using the Plant *Cis*-Acting Regulatory Element (<http://bioinformatics.psb.ugent.be/webtools/plantcare/html/>, accessed on 14 May 2024).

2.4. Chromosome Location, Ka/Ks Ratio, and Duplication Analyses of *NHX* Genes

The chromosomal locations of the identified *OsNHX* genes were determined using rice genome annotation information from the Phytozome database and visualized using the TB tool [49]. To gain insights into the duplication event of *OsNHX* genes and their evolutionary history, collinearity analysis of *OsNHX* genes was performed using the DupGen_finder tool on The Plant Genome and Gene Duplication Database (PlantGGD, <http://pdgd.njau.edu.cn:8080/>, accessed on 17 May 2024) and visualized with the default parameters of the MCScanX software in the TB tool version 2.142. The Ka/Ks ratios (non-synonymous/synonymous substitution rates) were calculated for pairs of duplicated *OsNHX* genes using MEGA 11 software to evaluate the selective pressure during their evolution [50].

2.5. Secondary Structure Analysis and the Three-Dimensional (3D) Structure Model Prediction

The secondary structure of *OsNHX* proteins was analyzed by NPS@: GOR4 (https://npsa-prabi.ibcp.fr/cgi-bin/npsa_automat.pl?page=/NPSA/npsa_gor4.html, accessed on 21 June 2024) [51]. The 3D structures of *OsNHX* proteins were created by using the I-TASSER tool (<https://zhanggroup.org/I-TASSER/>, accessed on 21 June 2024) [52]. The obtained results of the *OsNHX* protein were visualized by using the ICN3D tool (<https://www.ncbi.nlm.nih.gov/Structure/icn3d/>, accessed on 27 July 2024).

To detect the diversity and conservation of *OsNHX* proteins, we retrieved 16 *NHX* protein sequences from various organisms: *Oryza sativa* (*OsNHX*1–*OsNHX*7), *Arabidopsis thaliana* (*AtNHX*1, *AtNHX*6, *AtNHX*7, *AtNHX*8), *Solanum lycopersicum* (*SINHX*1), *Pyrococcus abyssi* (*PaNhaP*), *Escherichia coli* (*EcNhaA*), and *Thermus thermophilus* (*TtNapA*), and *Homo sapiens* (*SLC9A3_NHE3*). These proteins were aligned using the T-COFFEE server (<https://tcoffee.crg.eu/>, accessed on 21 June 2024) [53] to highlight the ND-motif and the amiloride binding site domain (FFI/LY/FLLPPI).

2.6. Comparative Analysis of Cis-Regulatory Elements and GO of *OsNHX* Genes

To identify *cis*-regulatory elements (CREs), we extracted 1500 bp upstream sequences (from the start codon) of *OsNHX* genes from the Phytozome V13 database and analyzed them using the New PLACE database [54]. Predicted CREs were classified into different groups based on their functions. These groups were visualized using the pheatmap and ggplot2 packages in R.

The GO Enrichment tool (<https://plantregmap.gao-lab.org/go.php>, accessed on 21 June 2024) was used to perform GO ontology (GO) analysis for *NHX* genes in rice. The TB tool version 2.142 was used to visualize the components and distributions of the annotated GO terms.

2.7. In Silico Analysis of *OsNHX* Gene Expression Profiles in Rice

The expression profiles of *OsNHX* genes were identified using publicly available transcriptomic data downloaded from NCBI GEO (<https://www.ncbi.nlm.nih.gov/geo/query/acc.cgi?acc=GSE60287>, accessed on 12 November 2024) [55]. These data include the following: GSM1470309 (IR64-Control), GSM1470311 (Pokkali-Control), GSM1470313 (IR64-Salinity stress), and GSM1470309 (Pokkali-Salinity stress). Here, the method FPKM (Fragments Per Kilobase of transcript per Million mapped reads) was used to normalized the abundance of transcripts across different samples. An *in silico* analysis was conducted based on transcriptomic data from two rice varieties, Pokkali and IR64, at seedling stage (14 days after being grown on reverse osmosis water-saturated cotton), and under salt stress at concentrations of 200 mM NaCl solution. Using the pheatmap function in R, a heat map was generated to illustrate the expression levels of the *OsNHX* genes under salt stress.

3. Results

3.1. Identification and Phylogenetic Analysis of *NHX* Genes in Rice

To identify the Na⁺/H⁺ s (s) in rice, the Hidden Markov Model (HMM) profile of the conserved Na⁺/H⁺ exchanger domain (PF00999) was used as a query to search against the Phytozome database. As a result, a total of 28 candidate *NHX* gene copies were detected in the rice genome. After removing redundant copies, seven non-redundant Na⁺/H⁺ genes were identified, which were correspondingly named *OsNHX1* to *OsNHX7* (Table 1a).

The key features of the *NHX* gene family in rice are listed in Table 1, including the gene locus s, protein sequence s, isoelectric s (pI), molecular s (MW), coding sequence s (CDS), and orthologous genes in *Arabidopsis*. Sequence analyses indicated that the genomic sequences of the *OsNHX* genes ranged from 4105 bp (*OsNHX2*) to 14,451 bp (*OsNHX7*). The number of exons in the coding sequence (CDS) ranged from 11 to 23, and the total length of the CDS was between 840 bp (*OsNHX6*) and 3477 bp (*OsNHX7*) (Table 1a).

The lengths of the 7 *OsNHX* proteins in rice range from 279 amino acids (aa) for *OsNHX6* to 1498 aa for *OsNHX7*, with an average of 511 aa. They have the lowest MW of 30.07 kDa (*OsNHX6*) and the highest MW of 127.91 kDa (*OsNHX7*), with an average of 65.03 kDa. The isoelectric point (pI) of the *OsNHX* proteins is between 5.60 and 8.23, with an average of 6.39.

All of the *OsNHX* proteins are typical transmembrane transporters and possess the Na⁺/H⁺ exchanger domain (PF00999). Generally, the number of transmembrane segments (TMs) ranged from 10 to 13, except for the *OsNHX6* protein, which has only 5 TMs (Table 1a, Figure S1).

Table 1. Some characteristics of *OsNHX* gene family in rice.

(a) Characteristics of <i>OsNHX</i> Gene Family Identified from the Rice Genome											
Gene Name	Gene Locus	Genomic Characteristic				Protein Characteristic				Arabidopsis Ortholog (% Identity)	
		Genomic Sequence (bp)	CDs Length (bp)	Exon/Intron	Protein Length (aa)	MW (kDa)	pI	TM	Signal Peptide		
<i>OsNHX1</i>	LOC_Os07g47100	4924	1608	14/13	535	59.07	7.77	12	No	AT3G05030 (75)	
<i>OsNHX2</i>	LOC_Os11g42790	4105	1638	13/12	545	59.91	8.23	12	No	AT3G05030 (72)	
<i>OsNHX3</i>	LOC_Os05g05590	6188	1635	14/13	544	59.64	7.17	12	No	AT3G05030 (70)	
<i>OsNHX4</i>	LOC_Os06g21360	4280	1587	13/12	528	58.22	6.31	11	No	AT5G55470 (63)	
<i>OsNHX5</i>	LOC_Os09g11450	10377	1650	18/17	549	60.39	5.75	11	Yes (1–17)	AT1G79610 (54)	
<i>OsNHX6</i>	LOC_Os09g30446	5309	840	11/10	279	30.07	5.60	5	Yes (1–17)	AT1G79610 (59)	
<i>OsNHX7</i>	LOC_Os12g44360	14451	3477	23/22	1148	127.91	6.77	13	No	AT2G01980 (64)	

(b) The number and phosphorylation sites (SP) of <i>OsNHX</i> proteins identified from the rice genome																
Protein name	SP			Unsp	PKC	CKI	PKA	CdC2	CKII	DNAPK	INSR	p38MAPK	CDK5	EGFR	ATM	SP for each protein
	Th	S	Tyr													
<i>OsNHX1</i>	154	28	4	49	83	42	2	7	1	0	1	0	0	1	0	186
<i>OsNHX2</i>	15	33	4	20	15	1	5	5	1	2	0	1	1	1	0	52
<i>OsNHX3</i>	12	30	1	14	15	0	6	3	2	1	0	1	0	0	1	43
<i>OsNHX4</i>	20	35	2	25	12	1	10	6	0	1	0	2	0	0	0	57
<i>OsNHX5</i>	13	30	4	18	9	0	5	5	3	4	2	0	1	0	0	47
<i>OsNHX6</i>	10	14	0	8	7	1	3	5	0	0	0	0	0	0	0	24
<i>OsNHX7</i>	32	63	9	45	23	3	12	9	4	3	4	0	1	0	0	104
Total	256	233	24	179	164	48	43	40	11	11	7	4	3	2	1	

Note: **Unsp:** Unspecified phosphorylation, **PKC:** Protein kinase C, **CKI:** Casein kinase 1, **PKA:** Protein kinase A, **CdC2:** Cell division cycle protein 2, **CKII:** Casein kinase 2, **DNAPK:** DNA dependent protein kinase, **INSR:** Insulin receptor precursor, **p38MAPK:** P38 Mitogen activated protein kinase, **CDK5:** Cyclin dependant kinase 5, **EGFR:** Epidermal growth factor receptor, **ATM:** Ataxia telangiectasia mutated.

The results of the signal peptide analysis showed that two proteins, OsNHX5 and OsNHX6, contained an N-terminal signal peptide (amino acid residues 1–17). This suggests that they are likely to be localized to endosomal compartments such as the trans-Golgi network/early endosome (TGN/EE) and prevacuolar compartment (PVC). Previous studies reported that signal peptides in these proteins are involved in the subcellular trafficking pathway, which are an important s of endosomal NHX proteins [23,56,57].

To identify orthologous genes, we aligned the amino acid sequences of the OsNHX proteins with those of the AtNHX proteins. The results showed that the *OsNHX1-3* gene group shares a single ortholog, AT3G05030. Similarly, two genes, *OsNHX5* and *OsNHX6*, also share a single ortholog, AT1G79610. In contrast, each of the genes, *OsNHX4* and *OsNHX7*, has its distinct orthologs, AT5G55470 and AT2G01980, respectively (Table 1a).

Phosphorylation analysis revealed a total of 513 phosphorylation sites across the 7 OsNHX protein sequences in rice. These sites can be categorized into three types of phosphorylation sites: serine (S), threonine (Thr), and tyrosine (Tyr). As shown in Table 1b, phosphorylation sites are dominated by Thr, indicating that Thr is a common phosphorylation site in the rice NHX protein family. Additionally, all OsNHX proteins are mostly phosphorylated with UNSP (179), PKC (164), and CKI (48), while only one phosphorylation site was detected for ATM.

To explore the evolutionary relationships of the NHX protein family across different plant species, we analyzed a total of 50 NHX protein sequences from 7 species: *Oryza sativa*, *Arabidopsis thaliana*, *Solanum lycopersicum*, *Cucurbita maxima*, *Lonicera japonica*, *Populus trichocarpa*, and *Sorghum bicolor*. The phylogenetic tree (Figure 1) divided these 50 NHX proteins into 3 clusters based on their subcellular localization: vacuolar membrane (Vac), endosomal membrane (Endo), and plasma membrane (PM). Among the clades, the Vac-NHX clade contained the majority of NHX proteins (33), followed by the Endo-NHX clade (9), and finally the PM-clade (8). In rice, the NHX protein family was also divided into three groups, including vacuolar NHX (*OsNHX1-4*), endosomal NHX (*OsNHX5* and *OsNHX6*), and plasma membrane NHX (only *OsNHX7*). Additionally, the *OsNHX* proteins tend to cluster closely with *SbNHXs* in the phylogenetic tree (Figure 1). This may be due to both *Oryza sativa* L. and *Sorghum bicolor* being members of the Poaceae family.

3.2. Chromosomal Location, Ka/Ks Ratio, and Gene Duplication Analysis

The distribution map of *OsNHX* genes was visualized based on the rice genome and an analysis of gene duplication events. Specifically, the 7 putative *OsNHX* genes were distributed across 6 chromosomes. *OsNHX5* and *OsNHX6* were located on chromosome 9, while *OsNHX1*, *OsNHX2*, *OsNHX3*, *OsNHX4*, and *OsNHX7* were found on chromosomes 7, 11, 5, 6, and 12, respectively (Figure 2).

The duplication of *OsNHX* genes was further investigated using the DupGen_finder tool on The Plant Genome and Gene Duplication Database (PlantGGD, <http://pdgd.njau.edu.cn:8080/>, accessed on 17 May 2024). In the rice genome, 5 duplication events (*OsNHX1/OsNHX2*, *OsNHX1/OsNHX3*, *OsNHX1/OsNHX4*, *OsNHX2/OsNHX6*, and *OsNHX5/OsNHX6*) involving 6 *OsNHX* genes were observed on chromosomes 5, 6, 7, 9, and 11 (Figure 2, Table 2). Among the *OsNHX* genes, *OsNHX1* is the common duplicated gene of three genes (*OsNHX2*, *OsNHX3*, and *OsNHX4*), while no duplication events were found in *OsNHX7*. According to Akram et al. (2020), two or more genes located on the same chromosome are referred to as tandem repeats, while segmental duplication refers to the presence of genes on different chromosomes [58]. In this study, the distance between the *OsNHX5* and *OsNHX6* genes is 12.16 Mb which is larger than 100 kb. Thus, there is no tandem duplication event in this case. Moreover, the results of the gene duplication analysis from PlantGGD show that five pairs of duplications (*OsNHX1/OsNHX2*,

OsNHX1/OsNHX3, *OsNHX1/OsNHX4*, *OsNHX2/OsNHX6*, and *OsNHX5/OsNHX6* are all classified as dispersed duplications (DSD) (Table 2).

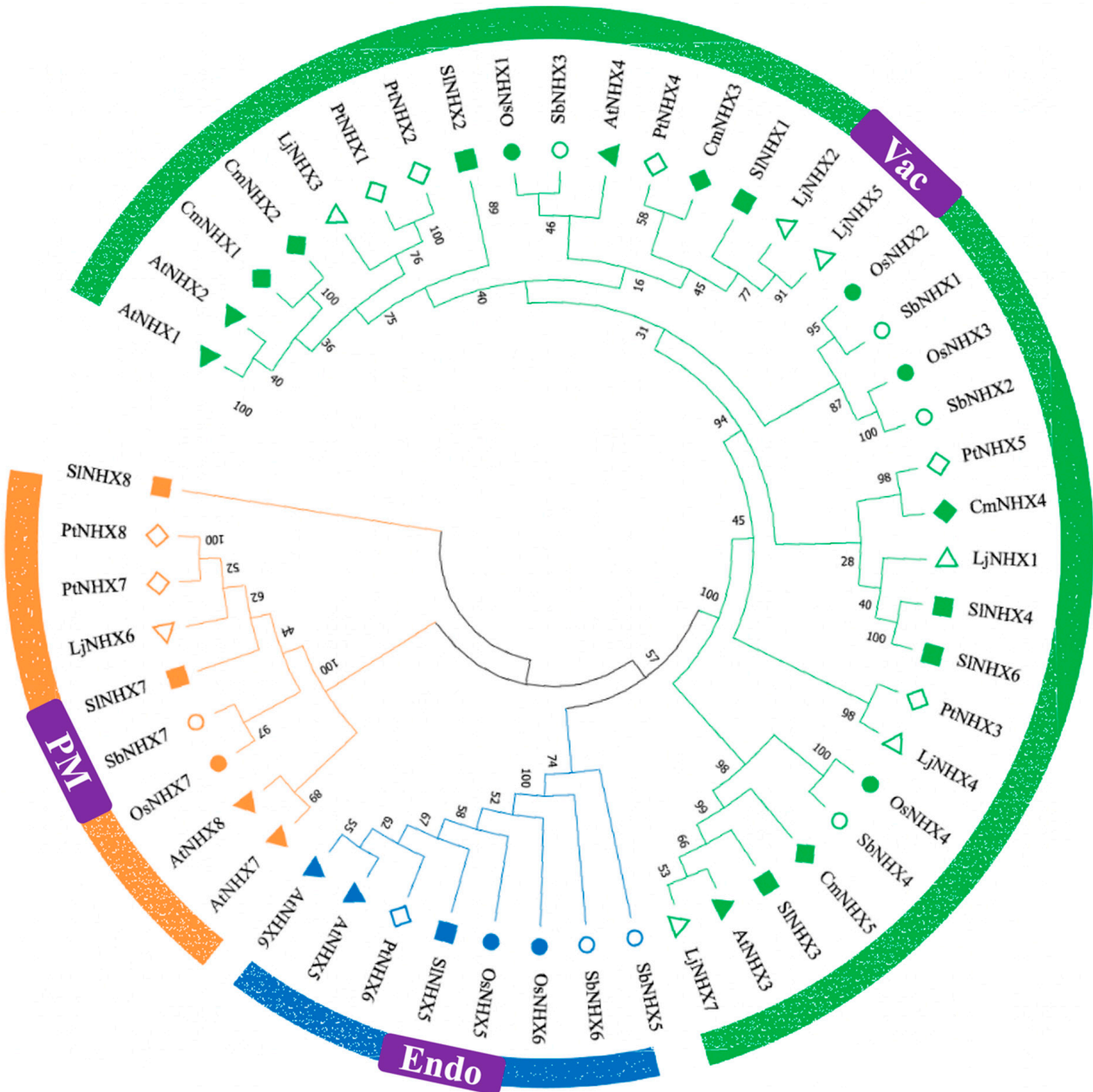


Figure 1. Phylogenetic relationships among NHX proteins from *Oryza sativa* (Os), *Arabidopsis thaliana* (At), *Solanum lycopersicum* (Sl), *Cucurbita maxima* (Cm), *Lonicera japonica* (Lj), *Populus trichocarpa* (Pt), and *Sorghum bicolor* (Sb). The phylogenetic tree was constructed using the amino acid sequences of selected NHX proteins. MEGA 11 software was employed with the MUSCLE alignment algorithm, the neighbor-joining (NJ) method, and 1000 bootstrap repetitions. Proteins from these plants are represented by distinct color clusters and shapes.

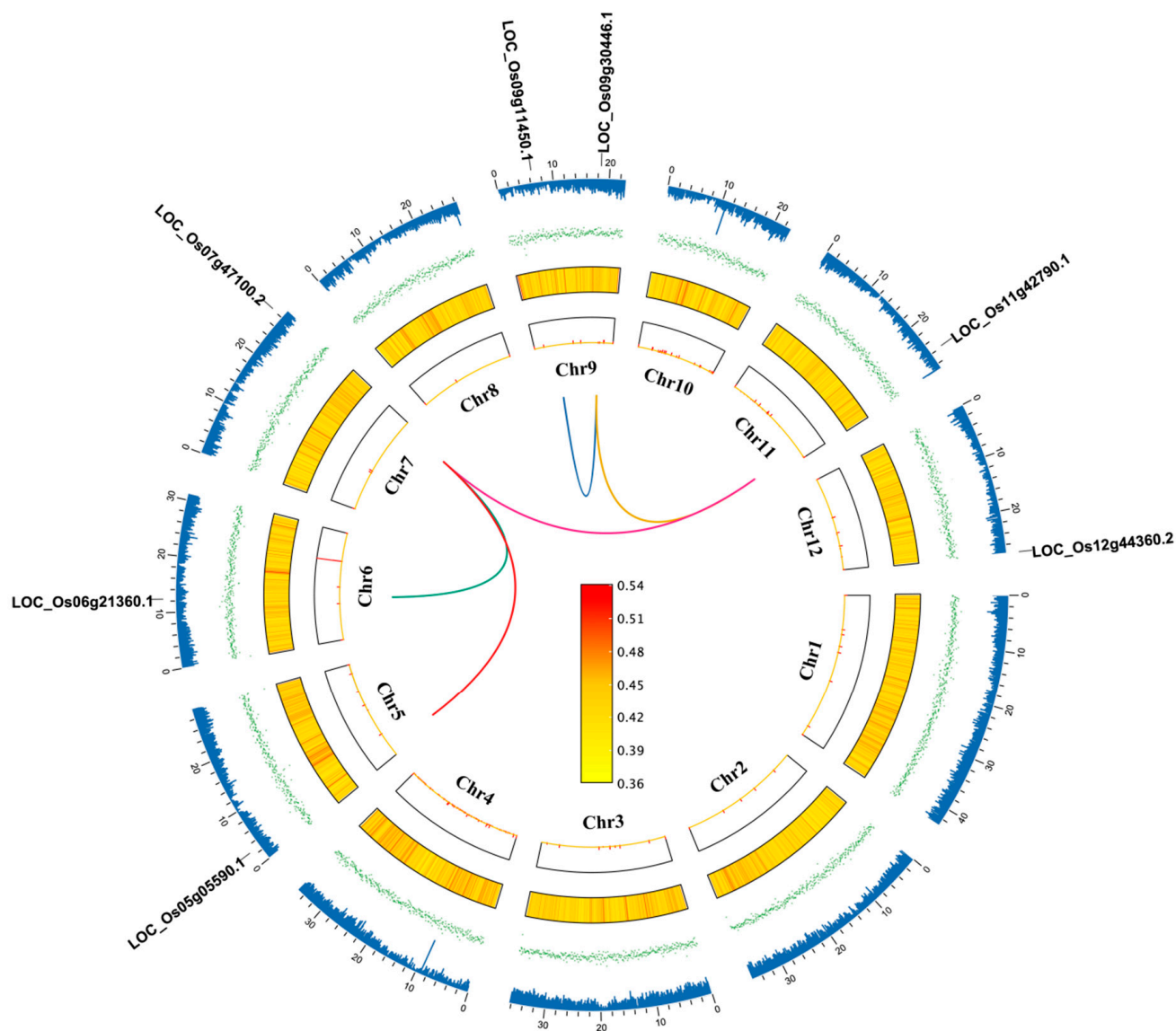


Figure 2. Schematic representation of the chromosomal distribution and synteny blocks of seven *OsNHX* genes. The circles, arranged from outer to inner, depict the *OsNHX* gene sites, gene density (blue), GC skew (green), GC ratio, N ratio, and chromosomes containing collinear blocks. Colored lines connect the duplicated *OsNHX* gene pairs.

Table 2. K_a/K_s ratio, duplication, and selection types of *OsNHX* genes in rice.

Gene Pairs	K_a	K_s	K_a/K_s	Duplicated Type	Selection Type
<i>OsNHX1-OsNHX2</i>	0.096	2.196	0.044	Dispersed duplication (DSD)	Purify
<i>OsNHX1-OsNHX3</i>	0.161	1.639	0.098	Dispersed duplication (DSD)	Purify
<i>OsNHX1-OsNHX4</i>	0.276	2.753	0.100	Dispersed duplication (DSD)	Purify
<i>OsNHX2-OsNHX6</i>	0.264	1.421	0.186	Dispersed duplication (DSD)	Purify
<i>OsNHX5-OsNHX6</i>	0.79	2.819	0.280	Dispersed duplication (DSD)	Purify

Abbreviations: K_a , the number of nonsynonymous substitutions per non-synonymous site; K_s , the number of synonymous substitutions per synonymous site.

The K_s and K_a values, calculated based the nucleotide sequences of the *NHX* genes, were used to explore the relationship between gene duplication events and natural selection. As shown in Table 2, the K_a/K_s ratios for five duplicated gene pairs were all less than 1, which indicated that the evolution of *OsNHX* gene pairs was predominantly driven by purifying selection and exhibited functional divergence after gene duplication [59].

3.3. Gene Structure and Characterization of Conserved Motif of NHX Proteins in Rice

By comparing the coding sequences with the genomic sequences of the *OsNHX* gene family, we identified the exon/intron structural features (Figure 3b), providing valuable insights into the functional roles of the genes and their evolutionary relationships. The number of exons in *OsNHX* genes ranged from 11 (*OsNHX6*) to 23 (*OsNHX7*), and genes within the same group exhibited similar intron/exon features. In general, most genes belonging to the Vac-NHX group (*OsNHX1-4*) possessed a similar exon/intron structure in terms of intron numbers and exon lengths, while the endosomal-NHX genes (*OsNHX5* and *OsNHX6*) varied from each other (Table 1 and Figure 3b).

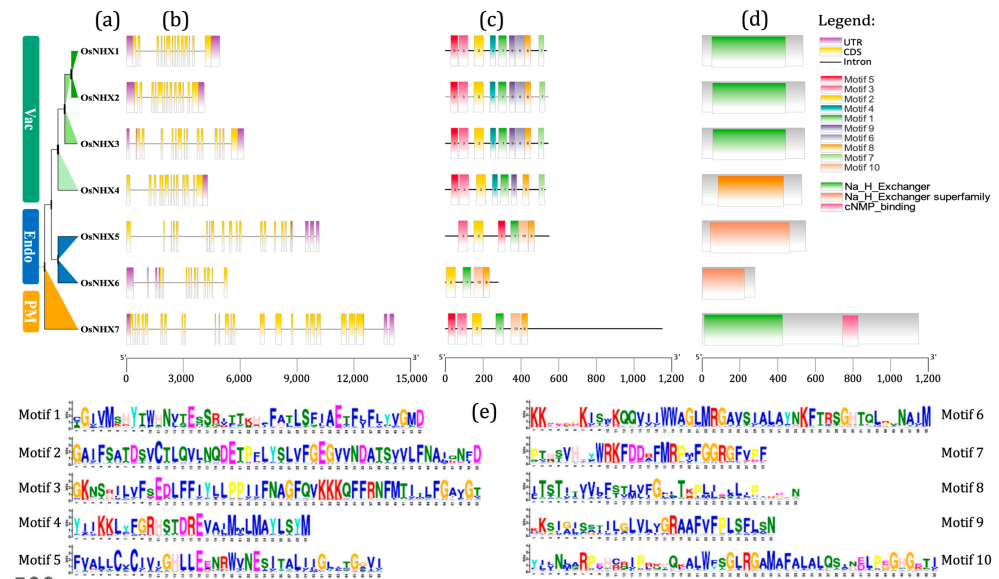


Figure 3. Analysis of *OsNHX* gene structure, protein motifs and domains. (a) Phylogenetic tree was constructed using the N-J method in MEGA11. (b) Exon/intron structures of the *OsNHX* genes were represented, with exons, introns, and UTRs depicted in yellow, black lines, and pale purple, respectively. (c) Motif distribution in *OsNHX* proteins was visualized by TB tool. (d) Conserved NHX protein domains. (e) Logo and amino acid composition of each motif were predicted by MEME tool.

The MEME server was used to predict different conserved motifs of *OsNHX* proteins, with the maximum number of motifs set at 10 (Figure 3c,e). It was found that some motifs were present in most NHX proteins (e.g., motifs 1, 2, 3, and 8), while some motifs were specific to certain proteins, such as motifs 6 (*OsNHX1-3* proteins) and 10 (*OsNHX5-7* proteins). This suggests that these specific motifs may have distinct functional roles in *OsNHX* proteins. Additionally, the NHX proteins within the same group (*OsNHX1-4* proteins) exhibited a similar pattern of motif distribution, indicating a close evolutionary relationship among members of this Vac group.

As shown in Figure 3d, *OsNHX7* contains two conserved domains: the Na⁺/H⁺ exchanger domain at the N-terminal and the cyclic nucleotide monophosphate (cNMP) binding domain at the C-terminal. The other six *OsNHX* proteins only have the Na⁺/H⁺ exchanger domain, which is responsible for the exchange of Na⁺ and H⁺ ions across the cell membrane or endomembrane systems, such as the vacuole and Golgi complex. Generally, the C-terminus of all *OsNHX* proteins is less conserved, is predicted to be hydrophilic, and plays crucial roles in channel activity regulation and protein trafficking through protein-protein interactions (Figure S1).

3.4. Feature of the Secondary and Three-Dimensional Structure of OsNHX Protein in Rice

The secondary structure of the OsNHX proteins was analyzed using the GOR4 online tool. The analysis revealed that randoms (more than 42.62%) were dominant among the structural types (random coil, extended strand, and alpha helix), except for OsNHX7, which had the largest proportion of alpha helices (45.21%) (Table S1).

In order to better understand the structural characteristics of OsNHX proteins, we generated 3D models using I-TASSER and visualized them with the iCn3D Structure Viewer (<https://www.ncbi.nlm.nih.gov/Structure/icn3d/>, accessed on 27 July 2024) (Figure 4).

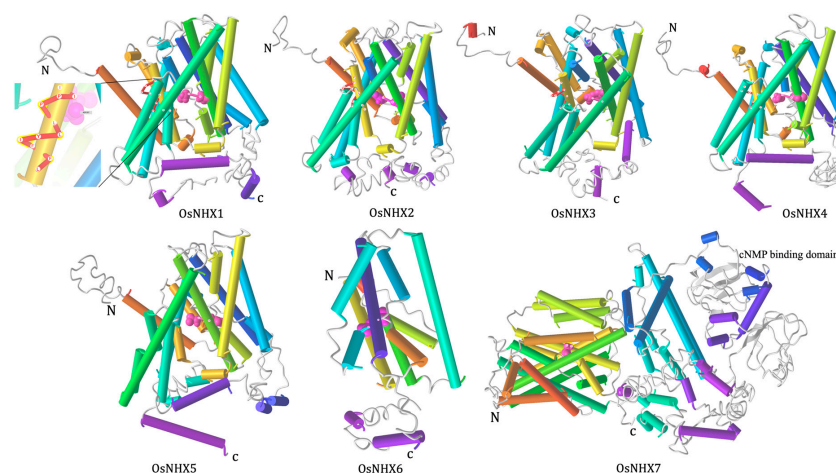


Figure 4. Predicted tertiary structures of OsNHX proteins in rice, showing N and C termini and domains. 3D models of OsNHX transporters viewed from the side. Amiloride binding sites are shown schematically in red, while ND motifs are represented as pink spheres (these sites are illustrated with zoomed-in views as in the OsNHX1 protein).

Homology searches showed that five of the seven OsNHX proteins share homology with the sodium proton antiporter NHE3-CHP1 from *Homo sapiens* (7x2uA), with a normalized Z-score greater than 3.30. OsNHX3 and OsNHX7 have homologous structures with the Cryo-EM structures of *Arabidopsis thaliana* SOS1, 7y3eA and 8jd9A, respectively (Table 3).

To assess these models, the C-score and TM-score were used to estimate the confidence of the predicted 3D structures and evaluate the structural similarity between two models, respectively. The C-score ranges from -5 to 2 , with higher scores indicating greater model reliability [52]. The TM-score, ranging from 0 to 1 , is a measure of structural similarity, with 1 indicating a perfect match between the two models. The modeling results revealed that the C-scores of the OsNHX proteins ranged from -0.93 to 0.04 , with the highest value observed in OsNHX1 (0.04) and the lowest in OsNHX5 (-0.93) (Table 3).

Table 3. The I-TASSER modeling parameters for OsNHX proteins 3D structure prediction.

Protein	PDB Template	Norm.Z-Score	C-Score	TM-Score	RMSD	Amiloride Binding Site (Start to End)	ND Motif (Start to End)
OsNHX1	7x2uA	5.90	0.04	0.72 ± 0.11	$7.4 \pm 4.2 \text{ \AA}$	84-FFIYLLPPI-93	186-ND-187
OsNHX2	7x2uA	5.03	-0.23	0.68 ± 0.12	$8.0 \pm 4.4 \text{ \AA}$	83-FFIYLLPPI-92	186-ND-187
OsNHX3	7y3eA	5.09	-0.29	0.68 ± 0.12	$8.2 \pm 4.4 \text{ \AA}$	85-FFIYLLPPI-94	187-ND-188
OsNHX4	7x2uA	4.94	-0.66	0.63 ± 0.14	$8.9 \pm 4.6 \text{ \AA}$	87-FFIYVLPPI-96	197-ND-198
OsNHX5	7x2uA	4.61	-0.93	0.60 ± 0.14	$9.7 \pm 4.6 \text{ \AA}$	-	184-ND-185
OsNHX6	7x2uA	3.30	-0.74	0.62 ± 0.14	$7.7 \pm 4.3 \text{ \AA}$	-	39-ND-40
OsNHX7	8jd9A	9.18	-0.03	0.71 ± 0.12	$9.3 \pm 4.6 \text{ \AA}$	-	175-ND-176

Abbreviation: PDB, protein database; RMSD, root mean square deviation; ND, asparagine, aspartic; - indicates no data available.

A summary of output parameters for predicting the 3D structures of OsNHX proteins, along with information on ND motifs and amiloride binding sites, is shown in Table 3. Accordingly, the amiloride binding site domain (FFIYLLPPI) is fully conserved in OsNHX1-3 and highly conserved in OsNHX4 (FFIYVLPPI), while this motif is not observed in OsNHX5-7. The ND motif, comprising asparagine (N) and aspartic acid (D) residues, is another important feature of OsNHX proteins and is present in all rice OsNHX family members. These motifs are characteristic of the CPA1 protein superfamily and are thought to be associated with Na⁺/H⁺ exchange across the cell membrane.

To further investigate the diversity and conservation of OsNHX proteins, we aligned various NHX proteins from humans, plants (*Oryza sativa*, *Arabidopsis thaliana*, and *Solanum lycopersicum*) and microbes (*E. coli*, *Pyrococcus abyssi*, and *Thermus thermophilus*) using the T-COFFEE tool (Figure 5 and Figure S2).

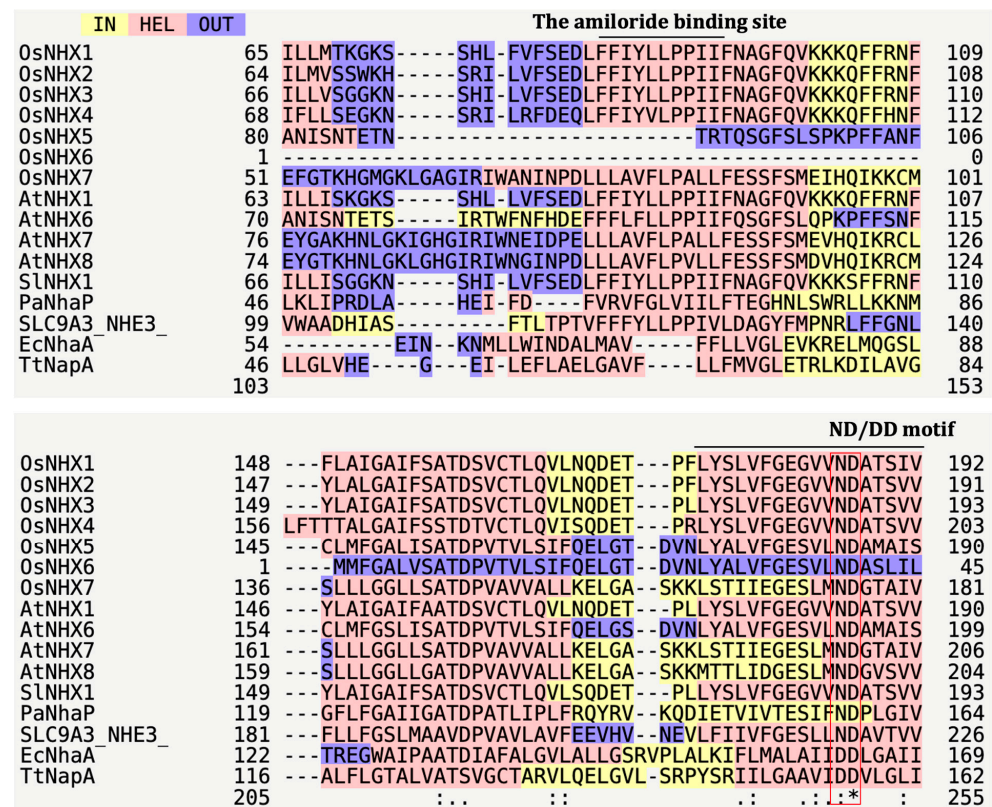


Figure 5. Characterization of amiloride binding sites and conserved ND motifs of NHX proteins were visualized by the T-COFFEE tool. Multiple sequence alignment of NHX proteins from *Oryza sativa* (OsNHX1-7); *Arabidopsis thaliana* (AtNHX1, AtNHX6, AtNHX7 and AtNHX8); *Solanum lycopersicum* (SlNHX1); *Pyrococcus abyssi* (PaNhaP); *E. coli* (EcNhaA); *Thermus thermophilus* (TtNapA), and *Homo sapiens* (SLC9A3_NHE3).

As shown in Figure 5, all proteins (NHX in plants and SLC9A3_NHE3 in humans) belonging to the CPA1 superfamily contain a conserved ND motif, while CPA2 proteins, such as EcNhaA and TtNapA, possess a DD motif. The amiloride binding site domain (FFIYLLPPI) is only observed in the Vac NHX cluster and is absent in other groups. This indicates that the ND motif is a main characteristic of the CPA1 protein. Therefore, in this study, all OsNHX proteins could be considered Na⁺/H⁺ antiporters (NHX) with an ND motif similar to that of the CPA1 protein.

3.5. GO Ontology Analysis and Cis-Regulatory Element Identification in Promoter of OsNHX Genes

In order to predict the functions of the seven *OsNHXs*, we performed a GO ontology analysis. As shown in Figure 6, *OsNHX* genes in rice were enriched in 57 GO terms, which were divided into 3 major groups including biological process (BP), cellular component (CC), and molecular function (MF) (Supplementary Table S2).

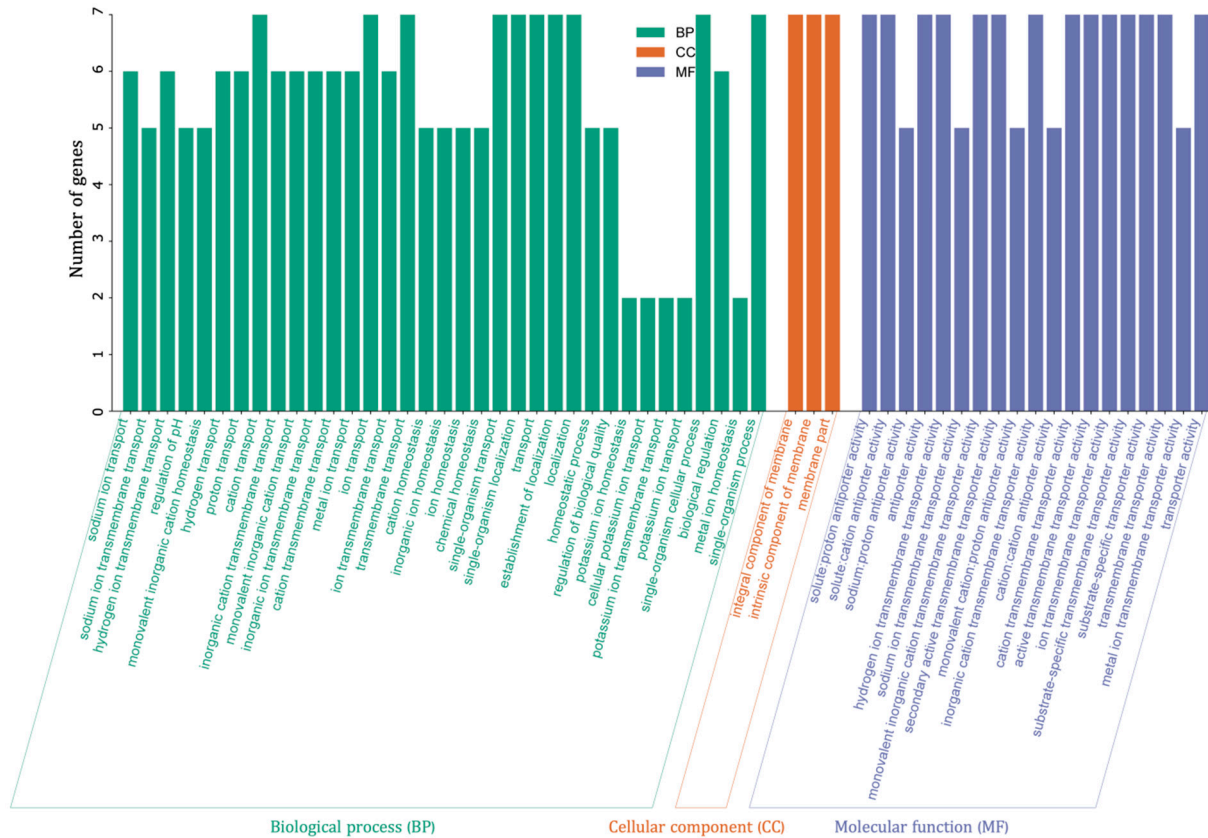


Figure 6. GO enrichment analysis of *OsNHX* genes in *Oryza sativa*. The results are grouped into three main categories: biological process (BP), cellular component (CC), and molecular function (MF). The y-axis shows the number of genes, while the x-axis shows the predicted functions.

The first group, BP, had the largest number of GO terms (34), followed by the MF group with 19 GO terms, while the CC group had the fewest, with only 3 GO terms. In general, the main GO terms observed in the BP category were related to cation transport, ion transport, transmembrane transport, sodium ion transport, and hydrogen ion transmembrane transport. In the CC group, although only three GO terms were enriched, all were associated with all seven *OsNHX* genes. For molecular function, the enriched GO terms in the MF category were primarily related to ion antiporter activity. Specifically, these included solute/proton antiporter activity (GO:0015299), solute/cation antiporter activity (GO:0015298), and hydrogen ion transmembrane transporter activity (GO:0015078). Additionally, Figure 5 shows enrichment for terms such as sodium/proton antiporter activity (GO:0015385), which is consistent with the role of *OsNHX* antiporters in sodium and hydrogen ion transport.

To explore the transcriptional regulation of rice *NHX* genes, we retrieved 1500 bp promoter sequences upstream of the “ATG” start codon from the Phytozome V13 database. We then used the New PLACE database to predict and analyze *cis*-regulatory elements (CREs) within these sequences. A total of 158 kinds of CREs were identified, randomly distributed across the promoter regions of the 7 rice *NHX* genes (Figure 7A, Supplementary Table S3).

Based on their biological functions, these CREs were classified into 11 groups, including those responsive to dehydration and salinity stress (17 CREs); heat and cold stress (7 CREs); light (22 CREs); other stresses (21 CREs); phytohormones (14 CREs); tissue/organelle-specific expression (27 CREs); pollen- and embryo-specific expression (9 CREs); binding site motifs (12 CREs); pathogen, elicitor, and wound responses (10 CREs); conserved motifs (11 CREs); and other functions (7 CREs). Among the 7 *OsNHX* genes, *OsNHX7* (359 CREs) had the highest number of *cis*-regulatory elements, followed by *OsNHX2* (358 CREs) and *OsNHX1* (349 CREs), while *OsNHX5* had the lowest number, at only 291 (Table S3).

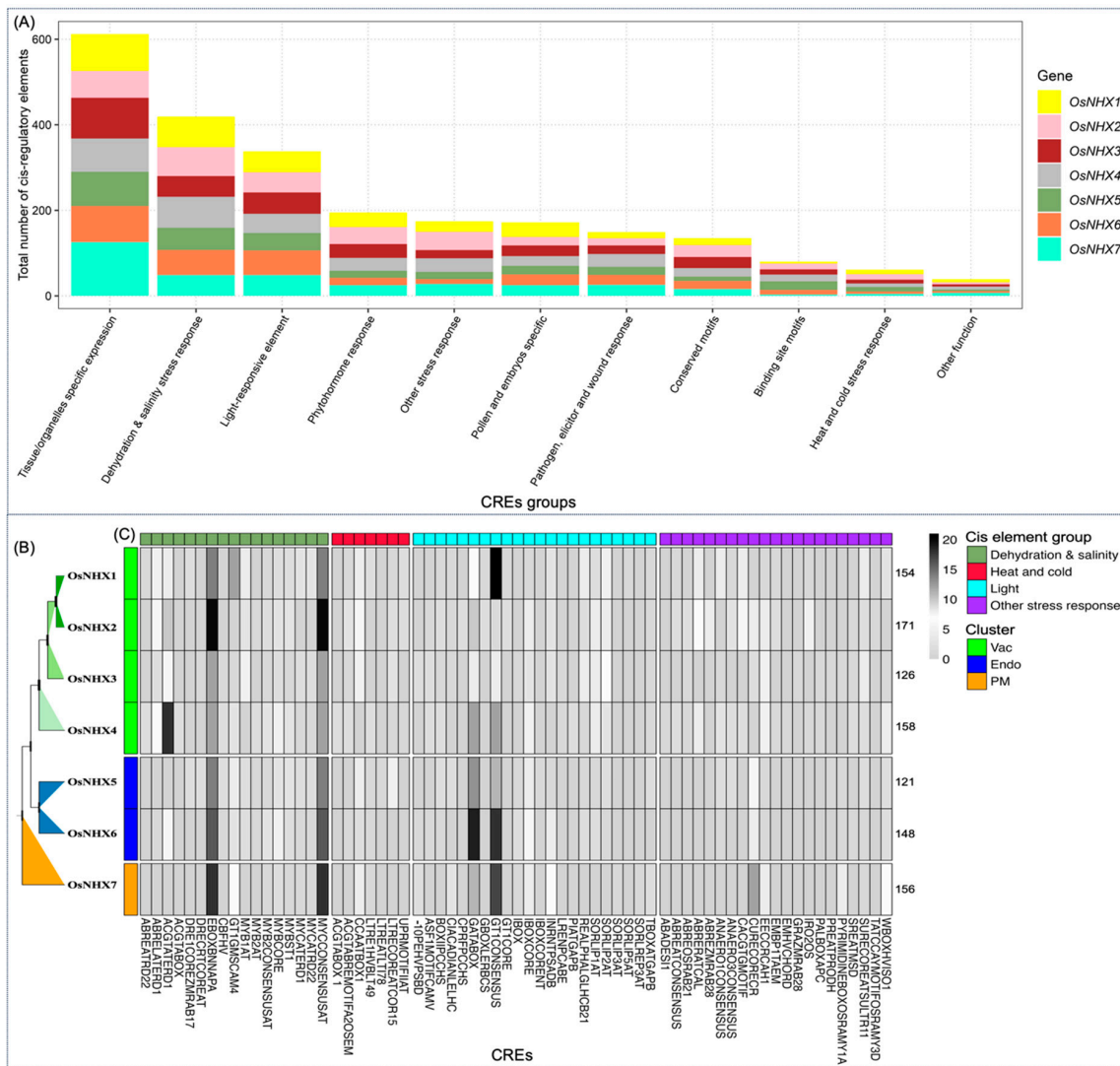


Figure 7. Analysis of *cis*-regulatory elements (CREs) in *OsNHX* genes. (A) The stacked bar chart of 11 CREs groups was identified from the PLACE PLANT database. (B) Phylogenetic tree was constructed using the N-J method in MEGA11. (C) Heatmap showing the frequency and distribution of stress-responsive CREs.

In this study, we focused on identifying stress-responsive elements, particularly those associated with dehydration and salinity stress (e.g., ABRE, MYB, MYC). Analysis of the 158 CREs revealed that 17 elements were involved in responses to dehydration and salinity stress, 7 in heat and cold stress responses, 22 in light responsiveness, and 21 in other stress responses (Figure 7B). Various light-responsive elements identified in the promoter regions of the *OsNHX* genes, such as GT1CONSENSUS, GATABOX, IBOXCORE, SORLIP1AT,

SORLIP2AT, and REALPHALGLHCB21. Notably, GATABOX and GT1CONSENSUS were highly abundant in all *OsNHX* genes, particularly in *OsNHX1* (21 CRE copies) (Table S3).

Despite comprising only 17 types of CREs, the group of *cis*-elements responding to dehydration and salinity stress (419 CRE copies) had the second highest total number of CRE copies, following the group for tissue/organelle-specific expression (612 CRE copies). Among these 17 CREs, EBOXBNNAPA/MYCCONSENSUSAT, GT1GMSCAM4, ACGTATERD1, and ABRELATERD1 occurred with high frequency in most *OsNHX* genes (Figure 7C).

3.6. Expression Profiles of Rice *NHXs* Under Salt Stress

Expression levels of *OsNHX* genes were quantified in Fragments Per Kilobase of exon model per Million mapped fragments (FPKM) and exhibited distinct expression patterns, ranging from 0.00 to 3.519 (Table S4, Figure 8).

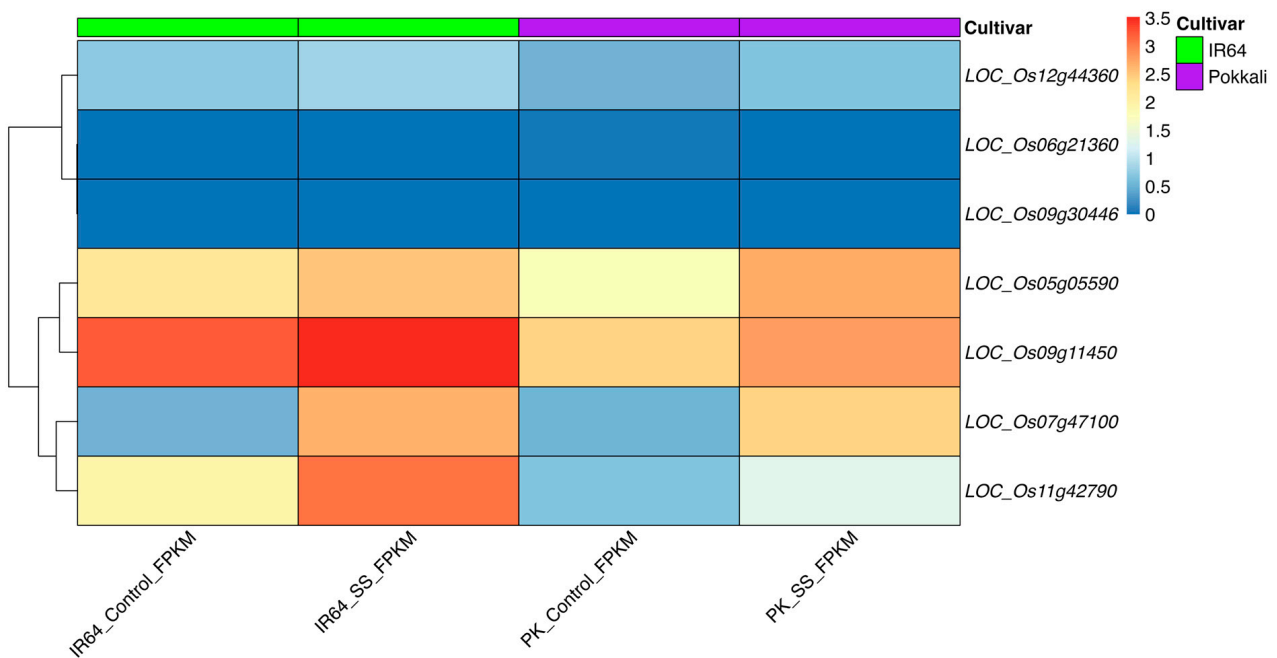


Figure 8. Heat map showing differential expression levels in FPKM of *OsNHX* genes under salt stress from two cultivars (IR64 and Pokkali). IR64_Control_FPKM: non-treated IR64; IR64_SS_FPKM: IR64 salt stress; PK_SS_FPKM: Pokkali salt stress; PK_Control_FPKM: non-treated Pokkali. The high expression level is indicated by the red color and the low expression level is shown by blue, with the color scale from 0 to 3.5 representing the FPKM expression values.

Gene expression analysis revealed that, out of the seven members of *OsNHX* genes, *OsNHX3* and *OsNHX5* were highly expressed in all rice samples, while *OsNHX6* showed the lowest expression in most varieties (Figure 8). Moreover, this gene showed minimal expression in the Pokkali cultivar.

In addition, it was observed that salt-treated rice varieties all had higher expression levels than non-treated varieties, especially in the *OsNHX1*, *OsNHX2*, *OsNHX3*, and *OsNHX5* genes (Figure 8). This demonstrates that salt stress can affect the expression of *OsNHX* genes in rice.

4. Discussion

The *NHX* gene family, which encodes a conserved Na^+/H^+ exchanger domain, is essential for various biological processes in plants, including responses to salt stress, cell expansion, and the regulation of pH and ion balance [11,35]. This highlights the crucial

role of the *NHX* gene family in plant physiology. Consequently, the identification and characterization of the *NHX* gene family have been extensively studied across various plant species. For example, eight *NHX* genes have been identified in two species, *Arabidopsis thaliana* and *Populus trichocarpa* [60,61]. Other species exhibit varying numbers of *NHX* genes, such as 5 in *Beta vulgaris* L. [62], 6 in *Vitis vinifera* [63], 7 in *Lonicera japonica* [45], 9 in *Cucurbita moschata* [64], and 25 in *Solanum tuberosum* L. [65]. The variation in the number of *NHX* genes across different species is influenced by gene duplication and loss events during evolution [62].

In this study, seven *OsNHX* genes were identified and characterized in the rice genome based on BLAST searches for the Na^+/H^+ exchanger domain (Table 1). Furthermore, gene structural features, phylogenetic relationships, genomic duplication, conserved domains, and CREs of rice *OsNHX* genes were analyzed at the genomic level using in silico methods.

The exon/intron structural diversity is an important feature in the evolution of gene families and provides additional evidence supporting phylogenetic classification. In rice, *OsNHX1*–*OsNHX4* genes have fewer exons (13–14) than *OsNHX5* (18) and *OsNHX7* (23). Similarly, in soybean, poplar, and sugar beet, the number of exons in the Vac-*NHX* cluster is also lower than that in the endosomal-*NHX* and PM-*NHX* clusters [60,62]. These results imply that *NHX* genes, particularly those in the Vac-*NHX* cluster, exhibit structural conservation among plant species.

Phylogenetic analysis (Figure 1) showed that *OsNHX* proteins are grouped into three clusters (Vac-, Endo-, and PM-clusters), similar to the classification of *NHX* protein families in other plants, as seen in previous phylogenetic classifications of *NHX*s in other species such as *Arabidopsis* [61], poplar [60], sugar beet [62], potato [65], and honeysuckle [45]. The function of *NHX* transporters is influenced by their subcellular localization. *NHX* protein members located on the plasma membrane and tonoplast help maintain ionic homeostasis by excluding and compartmentalizing excess Na^+ ions. In contrast, endomembrane-bound *NHX* proteins play a key role in cellular cargo trafficking, growth and development, and protein processing [23]. Signal peptides were only identified in the endo-*NHX* proteins (*OsNHX5* and *OsNHX6*) in rice (Table 1a), which may explain their role in the cellular cargo trafficking pathway [23,57].

It has been reported that gene duplication, a common phenomenon in plants, plays a crucial role in the emergence of new genes and their functional divergence [66,67]. Analysis of gene duplication events in the rice genome revealed that the paralogous pairs (*OsNHX1/OsNHX2*, *OsNHX1/OsNHX3*, *OsNHX1/OsNHX4*, *OsNHX2/OsNHX6*, and *OsNHX5/OsNHX6*) were generated by DSD duplication. However, our findings contrast with some reports that indicate most paralogous pairs are formed by fragment or tandem duplication [43,58,68,69]. DSD is one of the key drivers of gene family expansion, arising through mechanisms that remain poorly understood [70]. Previous reports have shown that salt stress can cause DNA damage [71,72]. Consequently, the expansion of genes involved in maintaining DNA and chromosome stability, including those associated with DSD, may represent an adaptive response of rice to salt-stressed environments. Functionally, gene duplication, such as DSD, can lead to neo-functionalization or sub-functionalization of duplicated genes [73], thereby potentially contributing to the diversification of gene functions and their roles in salinity tolerance.

The K_a/K_s ratio can be used to examine the selective pressure acting on the *OsNHX* gene family, including positive, negative, and neutral selection. In this study, all paralogous pairs exhibited a K_a/K_s ratio < 1 , suggesting that they underwent strong purifying selection (Table 2). Similar K_a/K_s ratios were also reported in tomato [43], cotton [74], tea [75], and wheat [69], further confirming the evolutionary conservation of these genes across species.

There are typically 10 to 12 transmembrane domains in most NHX proteins, which consist of approximately 550 amino acids and include a putative amiloride binding domain (FFI/LY/FLLPPI) in the third transmembrane domain, as reported in several studies [43,76]. This amiloride binding domain is well-known to be responsible for inhibiting the cation/H⁺ exchange of eukaryotic NHXs in the presence of amiloride [26,77]. However, not all NHX members possess these characteristics. For instance, OsNHX1-5 proteins have 11–12 transmembrane domains, while OsNHX6 has only 5. The OsNHX7 protein has the largest number of amino acids (1148) and transmembrane domains (13) (Table 1a). Notably, the conserved motif (FFIYL/VLPPI) was found only in the Vac-NHX cluster (OsNHX1-4), but not in the other groups (Table 3, Figure 4). This finding is in line with the results reported by Wu et al. (2019) [62]. However, some studies revealed that the amiloride binding domain was also observed in the endosomal-NHX group [43,76], while others reported that many NHX proteins do not contain the amiloride binding domain in their structure [76,77]. These contrasting findings suggest that the amiloride binding domain is not conserved in all species and that its sites and sequences may differ among species.

In this study, we detected the ND motif in all OsNHX members (Table 3, Figure 4). Accordingly, the high degree of conservation of the ND motif has been observed in various electroneutral CPA1 family members, including SINHX1 (N187-D188), PaNhaP (N158-D159), SLC9A3_NHE3 (N220-D221), and some members of the *Arabidopsis* NHX family (Figure 4). This motif is also exhibited in some species such as MjNhaP1 (N160-D161), PeNHX3 (N187-D188), and HsNHE1 (N266-D267) [78]. According to Masrati et al. (2018), the ND motif at the Nha-fold interacts with the TD-motif in TM4 to determine the substrate specificity of cation/proton exchangers of the CPA superfamily, suggesting a critical role for NHX activity [79]. Therefore, it can be said that the ND motif in the OsNHX protein family plays a critical role in Na⁺/H⁺ exchange and NHX antiporter activity, along with the amiloride binding domain.

There are various external environmental factors that can affect plant development and growth, including abiotic stresses such as drought, high temperatures, salinity, and metal toxicity [80] or biotic factors such as, pathogenic viruses, bacteria, fungi, and nematodes [81]. CRE elements are key control elements in the transcriptional regulation of genes, playing a crucial role in plant responses to environmental changes [82].

In this study, CRE groups related to tissue/organelle-specific expression (27 CREs) and stress response (67 CREs) are the most abundant in the promoters of *OsNHX* genes (Table S3). This demonstrates the important role of the *OsNHX* gene family in the growth, development, and stress tolerance of rice. We identified several *cis*-acting elements associated with salt and drought stress in the promoter region of the *OsNHX* genes, such as ABRELATERD1, MYBCORE, ACGTATERD1, GT1GMSCAM4, MYB2CONSENSUSAT, and MYCCONSENSUSAT [83]. The presence of MYB2CONSENSUSAT, MYBCORE, MYBST1, and MYCCONSENSUSAT in all *OsNHX* genes indicates that these elements are highly conserved in the *OsNHX* family. Additionally, several other *cis*-elements were also identified in the promoter regions of *OsNHX* genes, such as CCAATBOX1 (heat stress response) [84], GT1CONSENSUS (light response) [85], ARR1AT (hormone response) [86], GTGANTG10 (Pollen-specific element) [87], and WRKY71OS (pathogen-responsive) [88].

Cis-regulatory elements (CREs) are vital for gene regulation and influence how plants respond to environmental changes, ultimately affecting their growth [89]. Analysis of CREs in the *OsNHX* gene family suggests that these genes may be involved in various phytohormone, light, salt, drought, biotic, and other stress responses in rice plants, highlighting their crucial role in rice adaptation and survival.

Given the association of *OsNHX* genes with stress-responsive *cis*-acting elements, we proposed that their expression patterns would vary between contrasting rice cultivars

under salt stress. Thus, we analyzed the expression levels of *OsNHX* genes from two contrasting cultivars (IR64 and Pokkali) under salt stress at the seedling stage. In our study, the expression of *OsNHX1*, *OsNHX2*, *OsNHX3*, and *OsNHX5* differed between the rice cultivars and was increased by salt stress. These findings align with previous studies on *OsNHX* genes in rice [30]. Pokkali is a well-known salt-tolerant rice cultivar, while IR64 is salt-sensitive. This differential expression pattern suggests that Pokkali may have a more robust regulatory mechanism for activating *OsNHX* genes under salt stress, which contributes to its enhanced salt tolerance. In contrast, the lower expression of these genes in IR64 under similar conditions may reflect its limited ability to cope with salt stress.

Other research using transgenic methods confirmed that overexpression of *OsNHX1* enhanced salt tolerance in transgenic plants [36,90]. In addition, *OsNHX2*, *OsNHX4*, *OsNHX5*, *OsNHX3*, and *SOS1/OsNHX7* were observed to be highly expressed in salt-tolerant varieties such as Pokkali, JYGY-1, and Nagdong [35,91]. Taken together, these findings suggest that the expression of *OsNHX* genes in rice is intricately regulated in response to salt stress, exhibiting variations based on both the level of stress and the specific genotypes involved.

5. Conclusions

This study identified and characterized seven non-redundant *OsNHX* genes in the rice genome and provided a comprehensive analysis of their phylogenetic relationships, gene structure, duplication events, conserved protein domains, *cis*-regulatory elements, and expression profiles under salt stress in distinct cultivars. Phylogenetic analysis revealed that *OsNHX* genes are divided into three subgroups: Vac, Endo, and PM, based on their subcellular localization and evolutionary relationships. The presence of conserved ND motifs and amiloride binding domains in *OsNHX* proteins suggests a critical role of these genes in Na^+/H^+ exchange and salt tolerance. Additionally, CRE analysis highlighted the abundance of *cis*-elements associated with stress responses, particularly to salinity and dehydration, in the promoters of *OsNHX* genes. Notably, *OsNHX1*, *OsNHX2*, *OsNHX3*, and *OsNHX5* exhibited significantly higher expression under salt stress, highlighting their role in maintaining ion and pH homeostasis under salinity stress. The results of this study enhance our understanding of the functional diversity and crucial role of *OsNHX* genes in rice growth, development, and stress tolerance, paving the way for their targeted manipulation to improve salt tolerance.

Supplementary Materials: The following supporting information can be downloaded at: <https://www.mdpi.com/article/10.3390/ijpb16010006/s1>, Figure S1: Topological features of *OsNHX* proteins in rice; Figure S2: Multiple sequence alignment of *NHX* protein family from some organisms; Table S1: The secondary structure prediction of the members of *OsNHX* protein Family; Table S2: The GO enrichment analysis of all the 7 *OsNHX* genes; Table S3: Identification of *cis* elements in the promoter region of *OsNHX* genes; Table S4: Gene expression profiles of *OsNHX* genes under salt stress.

Author Contributions: Conceptualization, D.H.N., H.H.T.B. and V.N.B.; methodology, D.H.N., H.H.T.B., H.T.T.T. and L.T.T.D.; software, D.H.N. and T.K.V.; validation, D.H.N. and V.N.B.; formal analysis, D.H.N., H.H.T.B. and H.T.T.T.; visualization, D.H.N.; resources, H.H.T.B. and V.N.B.; data curation, H.H.T.B., L.T.T.D., H.T.T.T. and T.K.V.; writing—original draft preparation, D.H.N., H.H.T.B., L.T.T.D., H.T.T.T. and T.K.V.; writing—review and editing, D.H.N. and V.N.B.; supervision, D.H.N. and V.N.B.; project administration, V.N.B.; funding acquisition, H.H.T.B. and V.N.B. All authors have read and agreed to the published version of the manuscript.

Funding: This study was funded by project “Analysing the diversity, conservation and function of the NHX protein family in rice (*Oryza sativa* L.) by *in silico* method “ code MHN 2023-01.03 from Ha Noi Open University.

Institutional Review Board Statement: Not applicable.

Informed Consent Statement: Not applicable.

Data Availability Statement: Data are contained within the article and Supplementary Materials.

Conflicts of Interest: The authors declare that they have no conflicts of interest.

References

1. Munns, R.; Tester, M. Mechanisms of Salinity Tolerance. *Annu. Rev. Plant Biol.* **2008**, *59*, 651–681. [[CrossRef](#)]
2. van Zelm, E.; Zhang, Y.; Testerink, C. Salt Tolerance Mechanisms of Plants. *Annu. Rev. Plant Biol.* **2020**, *71*, 403–433. [[CrossRef](#)]
3. Colin, L.; Ruhnnow, F.; Zhu, J.-K.; Zhao, C.; Zhao, Y.; Persson, S. The Cell Biology of Primary Cell Walls during Salt Stress. *Plant Cell* **2022**, *35*, 201–217. [[CrossRef](#)]
4. Li, J.; Ma, M.; Sun, Y.; Lu, P.; Shi, H.; Guo, Z.; Zhu, H. Comparative Physiological and Transcriptome Profiles Uncover Salt Tolerance Mechanisms in Alfalfa. *Front. Plant Sci.* **2022**, *13*, 931619. [[CrossRef](#)]
5. Zhao, S.; Zhang, Q.; Liu, M.; Zhou, H.; Ma, C.; Wang, P. Regulation of Plant Responses to Salt Stress. *Int. J. Mol. Sci.* **2021**, *22*, 4609. [[CrossRef](#)] [[PubMed](#)]
6. Hasanuzzaman, M.; Bhuyan, M.H.M.B.; Zulfiqar, F.; Raza, A.; Mohsin, S.M.; Mahmud, J.A.; Fujita, M.; Fotopoulos, V. Reactive Oxygen Species and Antioxidant Defense in Plants under Abiotic Stress: Revisiting the Crucial Role of a Universal Defense Regulator. *Antioxidants* **2020**, *9*, 681. [[CrossRef](#)]
7. Atta, K.; Mondal, S.; Gorai, S.; Singh, A.P.; Kumari, A.; Ghosh, T.; Roy, A.; Hembram, S.; Gaikwad, D.J.; Mondal, S.; et al. Impacts of Salinity Stress on Crop Plants: Improving Salt Tolerance through Genetic and Molecular Dissection. *Front. Plant Sci.* **2023**, *14*, 1241736. [[CrossRef](#)] [[PubMed](#)]
8. Xiao, F.; Zhou, H. Plant Salt Response: Perception, Signaling, and Tolerance. *Front. Plant Sci.* **2023**, *13*, 1053699. [[CrossRef](#)]
9. Zhou, H.; Shi, H.; Yang, Y.; Feng, X.; Chen, X.; Xiao, F.; Lin, H.; Guo, Y. Insights into Plant Salt Stress Signaling and Tolerance. *J. Genet. Genom.* **2024**, *51*, 16–34. [[CrossRef](#)] [[PubMed](#)]
10. Yarra, R. The Wheat NHX Gene Family: Potential Role in Improving Salinity Stress Tolerance of Plants. *Plant Gene* **2019**, *18*, 100178. [[CrossRef](#)]
11. Bassil, E.; Coku, A.; Blumwald, E. Cellular Ion Homeostasis: Emerging Roles of Intracellular NHX Na⁺/H⁺ Antiporters in Plant Growth and Development. *J. Exp. Bot.* **2012**, *63*, 5727–5740. [[CrossRef](#)]
12. Deinlein, U.; Stephan, A.B.; Horie, T.; Luo, W.; Xu, G.; Schroeder, J.I. Plant Salt-Tolerance Mechanisms. *Trends Plant Sci.* **2014**, *19*, 371–379. [[CrossRef](#)]
13. Fan, W.; Deng, G.; Wang, H.; Zhang, H.; Zhang, P. Elevated Compartmentalization of Na⁺ into Vacuoles Improves Salt and Cold Stress Tolerance in Sweet Potato (*Ipomoea batatas*). *Physiol. Plant* **2015**, *154*, 560–571. [[CrossRef](#)]
14. Yamaguchi, T.; Hamamoto, S.; Uozumi, N. Sodium Transport System in Plant Cells. *Front. Plant Sci.* **2013**, *4*, 410. [[CrossRef](#)]
15. Garcíadeblás, B.; Senn, M.E.; Bañuelos, M.A.; Rodríguez-Navarro, A. Sodium Transport and HKT Transporters: The Rice Model. *Plant J.* **2003**, *34*, 788–801. [[CrossRef](#)] [[PubMed](#)]
16. Horie, T.; Yoshida, K.; Nakayama, H.; Yamada, K.; Oiki, S.; Shinmyo, A. Two Types of HKT Transporters with Different Properties of Na⁺ and K⁺ Transport in *Oryza Sativa*. *Plant J.* **2001**, *27*, 129–138. [[CrossRef](#)] [[PubMed](#)]
17. Assaha, D.V.M.; Ueda, A.; Saneoka, H.; Al-Yahyai, R.; Yaish, M.W. The Role of Na⁺ and K⁺ Transporters in Salt Stress Adaptation in Glycophytes. *Front. Physiol.* **2017**, *8*, 509. [[CrossRef](#)]
18. Feki, K.; Quintero, F.J.; Khoudi, H.; Leidi, E.O.; Masmoudi, K.; Pardo, J.M.; Brini, F. A Constitutively Active Form of a Durum Wheat Na⁺/H⁺ Antiporter SOS1 Confers High Salt Tolerance to Transgenic Arabidopsis. *Plant Cell Rep.* **2014**, *33*, 277–288. [[CrossRef](#)]
19. Chanroj, S.; Wang, G.; Venema, K.; Zhang, M.W.; Delwiche, C.F.; Sze, H. Conserved and Diversified Gene Families of Monovalent Cation/H⁺ Antiporters from Algae to Flowering Plants. *Front. Plant Sci.* **2012**, *3*, 17646. [[CrossRef](#)]
20. Ford, B.A.; Ernest, J.R.; Gendall, A.R. Identification and Characterization of Orthologs of AtNHX5 and AtNHX6 in Brassica Napus. *Front. Plant Sci.* **2012**, *3*, 208. [[CrossRef](#)]
21. Brett, C.L.; Donowitz, M.; Rao, R. Evolutionary Origins of Eukaryotic Sodium/Proton Exchangers. *Am. J. Physiol. Cell Physiol.* **2005**, *288*, C223–C239. [[CrossRef](#)]
22. Saier, M.H.; Reddy, V.S.; Tsu, B.V.; Ahmed, M.S.; Li, C.; Moreno-Hagelsieb, G. The Transporter Classification Database (TCDB): Recent Advances. *Nucleic Acids Res.* **2016**, *44*, D372–D379. [[CrossRef](#)]

23. An, R.; Chen, Q.-J.; Chai, M.-F.; Lu, P.-L.; Su, Z.; Qin, Z.-X.; Chen, J.; Wang, X.-C. AtNHX8, a Member of the Monovalent Cation:Proton Antiporter-1 Family in Arabidopsis Thaliana, Encodes a Putative Li⁺/H⁺ Antiporter. *Plant J.* **2007**, *49*, 718–728. [[CrossRef](#)]
24. Bassil, E.; Ohto, M.; Esumi, T.; Tajima, H.; Zhu, Z.; Cagnac, O.; Belmonte, M.; Peleg, Z.; Yamaguchi, T.; Blumwald, E. The Arabidopsis Intracellular Na⁺/H⁺ Antiporters NHX5 and NHX6 Are Endosome Associated and Necessary for Plant Growth and Development[w]. *Plant Cell* **2011**, *23*, 224–239. [[CrossRef](#)] [[PubMed](#)]
25. Pardo, J.M.; Cubero, B.; Leidi, E.O.; Quintero, F.J. Alkali Cation Exchangers: Roles in Cellular Homeostasis and Stress Tolerance. *J. Exp. Bot.* **2006**, *57*, 1181–1199. [[CrossRef](#)]
26. Yamaguchi, T.; Apse, M.P.; Shi, H.; Blumwald, E. Topological Analysis of a Plant Vacuolar Na⁺/H⁺ Antiporter Reveals a Luminal C Terminus That Regulates Antiporter Cation Selectivity. *Proc. Natl. Acad. Sci. USA* **2003**, *100*, 12510–12515. [[CrossRef](#)] [[PubMed](#)]
27. Punta, M.; Coghill, P.C.; Eberhardt, R.Y.; Mistry, J.; Tate, J.; Boursnell, C.; Pang, N.; Forslund, K.; Ceric, G.; Clements, J.; et al. The Pfam Protein Families Database. *Nucleic Acids Res.* **2012**, *40*, D290–D301. [[CrossRef](#)] [[PubMed](#)]
28. Aharon, G.S.; Apse, M.P.; Duan, S.; Hua, X.; Blumwald, E. Characterization of a Family of Vacuolar Na⁺/H⁺ Antiporters in Arabidopsis Thaliana. *Plant Soil.* **2003**, *253*, 245–256. [[CrossRef](#)]
29. Shi, H.; Ishitani, M.; Kim, C.; Zhu, J.-K. The Arabidopsis Thaliana Salt Tolerance Gene SOS1 Encodes a Putative Na⁺/H⁺ Antiporter. *Proc. Natl. Acad. Sci. USA* **2000**, *97*, 6896–6901. [[CrossRef](#)]
30. Fukuda, A.; Nakamura, A.; Hara, N.; Toki, S.; Tanaka, Y. Molecular and Functional Analyses of Rice NHX-Type Na⁺/H⁺ Antiporter Genes. *Planta* **2011**, *233*, 175–188. [[CrossRef](#)] [[PubMed](#)]
31. Wu, Y.-Y.; Chen, Q.-J.; Chen, M.; Chen, J.; Wang, X.-C. Salt-Tolerant Transgenic Perennial Ryegrass (*Lolium perenne* L.) Obtained by *Agrobacterium tumefaciens*-Mediated Transformation of the Vacuolar Na⁺/H⁺ Antiporter Gene. *Plant Sci.* **2005**, *169*, 65–73. [[CrossRef](#)]
32. Lu, W.; Guo, C.; Li, X.; Duan, W.; Ma, C.; Zhao, M.; Gu, J.; Du, X.; Liu, Z.; Xiao, K. Overexpression of TaNHX3, a Vacuolar Na⁺/H⁺ Antiporter Gene in Wheat, Enhances Salt Stress Tolerance in Tobacco by Improving Related Physiological Processes. *Plant Physiol. Biochem.* **2014**, *76*, 17–28. [[CrossRef](#)]
33. Leidi, E.O.; Barragán, V.; Rubio, L.; El-Hamdaoui, A.; Ruiz, M.T.; Cubero, B.; Fernández, J.A.; Bressan, R.A.; Hasegawa, P.M.; Quintero, F.J.; et al. The AtNHX1 Exchanger Mediates Potassium Compartmentation in Vacuoles of Transgenic Tomato. *Plant J.* **2010**, *61*, 495–506. [[CrossRef](#)]
34. Li, W.; Wang, D.; Jin, T.; Chang, Q.; Yin, D.; Xu, S.; Liu, B.; Liu, L. The Vacuolar Na⁺/H⁺ Antiporter Gene SsNHX1 from the Halophyte *Salsola Soda* Confers Salt Tolerance in Transgenic Alfalfa (*Medicago sativa* L.). *Plant Mol. Biol. Rep.* **2011**, *29*, 278–290. [[CrossRef](#)]
35. Farooq, M.; Park, J.-R.; Jang, Y.-H.; Kim, E.-G.; Kim, K.-M. Rice Cultivars Under Salt Stress Show Differential Expression of Genes Related to the Regulation of Na⁺/K⁺ Balance. *Front. Plant Sci.* **2021**, *12*, 680131. [[CrossRef](#)] [[PubMed](#)]
36. Fukuda, A.; Nakamura, A.; Tagiri, A.; Tanaka, H.; Miyao, A.; Hirochika, H.; Tanaka, Y. Function, Intracellular Localization and the Importance in Salt Tolerance of a Vacuolar Na⁽⁺⁾/H⁽⁺⁾ Antiporter from Rice. *Plant Cell Physiol.* **2004**, *45*, 146–159. [[CrossRef](#)]
37. Sreedasyam, A.; Plott, C.; Hossain, M.S.; Lovell, J.T.; Grimwood, J.; Jenkins, J.W.; Daum, C.; Barry, K.; Carlson, J.; Shu, S.; et al. JGI Plant Gene Atlas: An Updateable Transcriptome Resource to Improve Functional Gene Descriptions across the Plant Kingdom. *Nucleic Acids Res.* **2023**, *51*, 8383–8401. [[CrossRef](#)] [[PubMed](#)]
38. Potter, S.C.; Luciani, A.; Eddy, S.R.; Park, Y.; Lopez, R.; Finn, R.D. HMMER Web Server: 2018 Update. *Nucleic Acids Res.* **2018**, *46*, W200–W204. [[CrossRef](#)]
39. Letunic, I.; Khedkar, S.; Bork, P. SMART: Recent Updates, New Developments and Status in 2020. *Nucleic Acids Res.* **2021**, *49*, D458–D460. [[CrossRef](#)] [[PubMed](#)]
40. Wang, J.; Chitsaz, F.; Derbyshire, M.K.; Gonzales, N.R.; Gwadz, M.; Lu, S.; Marchler, G.H.; Song, J.S.; Thanki, N.; Yamashita, R.A.; et al. The Conserved Domain Database in 2023. *Nucleic Acids Res.* **2023**, *51*, D384–D388. [[CrossRef](#)] [[PubMed](#)]
41. Käll, L.; Krogh, A.; Sonnhammer, E.L.L. A Combined Transmembrane Topology and Signal Peptide Prediction Method. *J. Mol. Biol.* **2004**, *338*, 1027–1036. [[CrossRef](#)]
42. Blom, N.; Sicheritz-Pontén, T.; Gupta, R.; Gammeltoft, S.; Brunak, S. Prediction of Post-Translational Glycosylation and Phosphorylation of Proteins from the Amino Acid Sequence. *Proteomics* **2004**, *4*, 1633–1649. [[CrossRef](#)]
43. Cavusoglu, E.; Sari, U.; Tiryaki, I. Genome-wide Identification and Expression Analysis of Na⁺/H⁺ Antiporter (NHX) Genes in Tomato under Salt Stress. *Plant Direct* **2023**, *7*, e543. [[CrossRef](#)]
44. Hima Kumari, P.; Anil Kumar, S.; Ramesh, K.; Sudhakar Reddy, P.; Nagaraju, M.; Bhanu Prakash, A.; Shah, T.; Henderson, A.; Srivastava, R.K.; Rajasheker, G.; et al. Genome-Wide Identification and Analysis of Arabidopsis Sodium Proton Antiporter (NHX) and Human Sodium Proton Exchanger (NHE) Homologs in Sorghum Bicolor. *Genes* **2018**, *9*, 236. [[CrossRef](#)] [[PubMed](#)]
45. Huang, L.; Li, Z.; Sun, C.; Yin, S.; Wang, B.; Duan, T.; Liu, Y.; Li, J.; Pu, G. Genome-Wide Identification, Molecular Characterization, and Gene Expression Analyses of Honeysuckle NHX Antiporters Suggest Their Involvement in Salt Stress Adaptation. *PeerJ* **2022**, *10*, e13214. [[CrossRef](#)] [[PubMed](#)]

46. Tamura, K.; Stecher, G.; Kumar, S. MEGA11: Molecular Evolutionary Genetics Analysis Version 11. *Mol. Biol. Evol.* **2021**, *38*, 3022–3027. [[CrossRef](#)]
47. Hu, B.; Jin, J.; Guo, A.-Y.; Zhang, H.; Luo, J.; Gao, G. GSDS 2.0: An Upgraded Gene Feature Visualization Server. *Bioinformatics* **2015**, *31*, 1296–1297. [[CrossRef](#)]
48. Bailey, T.L.; Boden, M.; Buske, F.A.; Frith, M.; Grant, C.E.; Clementi, L.; Ren, J.; Li, W.W.; Noble, W.S. MEME Suite: Tools for Motif Discovery and Searching. *Nucleic Acids Res.* **2009**, *37*, W202–W208. [[CrossRef](#)]
49. Chen, C.; Chen, H.; Zhang, Y.; Thomas, H.R.; Frank, M.H.; He, Y.; Xia, R. TBtools: An Integrative Toolkit Developed for Interactive Analyses of Big Biological Data. *Mol. Plant* **2020**, *13*, 1194–1202. [[CrossRef](#)] [[PubMed](#)]
50. Zhang, Z.; Li, J.; Yu, J. Computing Ka and Ks with a Consideration of Unequal Transitional Substitutions. *BMC Evol. Biol.* **2006**, *6*, 44. [[CrossRef](#)]
51. Combet, C.; Blanchet, C.; Geourjon, C.; Deléage, G. NPS@: Network Protein Sequence Analysis. *Trends Biochem. Sci.* **2000**, *25*, 147–150. [[CrossRef](#)] [[PubMed](#)]
52. Yang, J.; Zhang, Y. Protein Structure and Function Prediction Using I-TASSER. *Curr. Protoc. Bioinform.* **2015**, *52*, 5.8.1–5.8.15. [[CrossRef](#)] [[PubMed](#)]
53. Di Tommaso, P.; Moretti, S.; Xenarios, I.; Orobítz, M.; Montanyola, A.; Chang, J.-M.; Taly, J.-F.; Notredame, C. T-Coffee: A Web Server for the Multiple Sequence Alignment of Protein and RNA Sequences Using Structural Information and Homology Extension. *Nucleic Acids Res.* **2011**, *39*, W13–W17. [[CrossRef](#)]
54. Higo, K.; Ugawa, Y.; Iwamoto, M.; Korenaga, T. Plant Cis-Acting Regulatory DNA Elements (PLACE) Database: 1999. *Nucleic Acids Res.* **1999**, *27*, 297–300. [[CrossRef](#)] [[PubMed](#)]
55. Garg, R.; Narayana Chevala, V.V.S.; Shankar, R.; Jain, M. Divergent DNA Methylation Patterns Associated with Gene Expression in Rice Cultivars with Contrasting Drought and Salinity Stress Response. *Sci. Rep.* **2015**, *5*, 14922. [[CrossRef](#)]
56. Miyazaki, E.; Sakaguchi, M.; Wakabayashi, S.; Shigekawa, M.; Mihara, K. NHE6 Protein Possesses a Signal Peptide Destined for Endoplasmic Reticulum Membrane and Localizes in Secretory Organelles of the Cell*. *J. Biol. Chem.* **2001**, *276*, 49221–49227. [[CrossRef](#)]
57. Reguera, M.; Bassil, E.; Tajima, H.; Wimmer, M.; Chanoca, A.; Otegui, M.S.; Paris, N.; Blumwald, E. pH Regulation by NHX-Type Antiporters Is Required for Receptor-Mediated Protein Trafficking to the Vacuole in Arabidopsis. *Plant Cell* **2015**, *27*, 1200–1217. [[CrossRef](#)]
58. Akram, U.; Song, Y.; Liang, C.; Abid, M.A.; Askari, M.; Myat, A.A.; Abbas, M.; Malik, W.; Ali, Z.; Guo, S.; et al. Genome-Wide Characterization and Expression Analysis of NHX Gene Family under Salinity Stress in *Gossypium Barbadosense* and Its Comparison with *Gossypium Hirsutum*. *Genes* **2020**, *11*, 803. [[CrossRef](#)] [[PubMed](#)]
59. Lynch, M.; Conery, J.S. The Evolutionary Fate and Consequences of Duplicate Genes. *Science* **2000**, *290*, 1151–1155. [[CrossRef](#)]
60. Tian, F.; Chang, E.; Li, Y.; Sun, P.; Hu, J.; Zhang, J. Expression and Integrated Network Analyses Revealed Functional Divergence of NHX-Type Na⁺/H⁺ Exchanger Genes in Poplar. *Sci. Rep.* **2017**, *7*, 2607. [[CrossRef](#)] [[PubMed](#)]
61. Yokoi, S.; Quintero, F.J.; Cubero, B.; Ruiz, M.T.; Bressan, R.A.; Hasegawa, P.M.; Pardo, J.M. Differential Expression and Function of Arabidopsis Thaliana NHX Na⁺/H⁺ Antiporters in the Salt Stress Response. *Plant J.* **2002**, *30*, 529–539. [[CrossRef](#)] [[PubMed](#)]
62. Wu, G.-Q.; Wang, J.-L.; Li, S.-J. Genome-Wide Identification of Na⁺/H⁺ Antiporter (NHX) Genes in Sugar Beet (*Beta vulgaris* L.) and Their Regulated Expression under Salt Stress. *Genes* **2019**, *10*, 401. [[CrossRef](#)] [[PubMed](#)]
63. Ayadi, M.; Martins, V.; Ben Ayed, R.; Jbir, R.; Feki, M.; Mzid, R.; Géros, H.; Aifa, S.; Hanana, M. Genome Wide Identification, Molecular Characterization, and Gene Expression Analyses of Grapevine NHX Antiporters Suggest Their Involvement in Growth, Ripening, Seed Dormancy, and Stress Response. *Biochem. Genet.* **2020**, *58*, 102–128. [[CrossRef](#)]
64. Shen, C.; Yuan, J.; Li, X.; Chen, R.; Li, D.; Wang, F.; Liu, X.; Li, X. Genome-Wide Identification of NHX (Na⁺/H⁺ Antiporter) Gene Family in *Cucurbita* L. and Functional Analysis of CmoNHX1 under Salt Stress. *Front. Plant Sci.* **2023**, *14*, 1136810. [[CrossRef](#)] [[PubMed](#)]
65. Yihong, J.; Zhen, L.; Chang, L.; Ziyang, S.; Ning, Z.; Meiqing, S.; Yuhui, L.; Lei, W. Genome-Wide Identification and Drought Stress-Induced Expression Analysis of the NHX Gene Family in Potato. *Front. Genet.* **2024**, *15*, 1396375. [[CrossRef](#)]
66. Chen, H.; Chen, X.; Wu, B.; Yuan, X.; Zhang, H.; Cui, X.; Liu, X. Whole-Genome Identification and Expression Analysis of K⁺ Efflux Antiporter (KEA) and Na⁺/H⁺ Antiporter (NHX) Families under Abiotic Stress in Soybean. *J. Integr. Agric.* **2015**, *14*, 1171–1183. [[CrossRef](#)]
67. Conant, G.C.; Wolfe, K.H. Turning a Hobby into a Job: How Duplicated Genes Find New Functions. *Nat. Rev. Genet.* **2008**, *9*, 938–950. [[CrossRef](#)]
68. Liu, H.; Wang, K.; Mei, Q.; Wang, X.; Yang, J.; Ma, F.; Mao, K. Genome-Wide Analysis of the *Actinidia chinensis* NHX Family and Characterization of the Roles of *AcNHX3* and *AcNHX7* in Regulating Salt Tolerance in *Arabidopsis*. *Environ. Exp. Bot.* **2023**, *214*, 105477. [[CrossRef](#)]
69. Sharma, P.; Mishra, S.; Pandey, B.; Singh, G. Genome-Wide Identification and Expression Analysis of the NHX Gene Family under Salt Stress in Wheat (*Triticum aestivum* L.). *Front. Plant Sci.* **2023**, *14*, 1266699. [[CrossRef](#)]

70. Ganko, E.W.; Meyers, B.C.; Vision, T.J. Divergence in Expression between Duplicated Genes in Arabidopsis. *Mol. Biol. Evol.* **2007**, *24*, 2298–2309. [[CrossRef](#)]
71. Ahmad, R.; Hussain, S.; Anjum, M.A.; Khalid, M.F.; Saqib, M.; Zakir, I.; Hassan, A.; Fahad, S.; Ahmad, S. Oxidative Stress and Antioxidant Defense Mechanisms in Plants Under Salt Stress. In *Plant Abiotic Stress Tolerance: Agronomic, Molecular and Biotechnological Approaches*; Hasanuzzaman, M., Hakeem, K.R., Nahar, K., Alharby, H.F., Eds.; Springer International Publishing: Cham, Switzerland, 2019; pp. 191–205. ISBN 978-3-030-06118-0.
72. Vinocur, B.; Altman, A. Recent Advances in Engineering Plant Tolerance to Abiotic Stress: Achievements and Limitations. *Curr. Opin. Biotechnol.* **2005**, *16*, 123–132. [[CrossRef](#)] [[PubMed](#)]
73. Chen, H.; Zhang, Y.; Feng, S. Whole-Genome and Dispersed Duplication, Including Transposed Duplication, Jointly Advance the Evolution of TLP Genes in Seven Representative Poaceae Lineages. *BMC Genom.* **2023**, *24*, 290. [[CrossRef](#)]
74. Fu, X.; Lu, Z.; Wei, H.; Zhang, J.; Yang, X.; Wu, A.; Ma, L.; Kang, M.; Lu, J.; Wang, H.; et al. Genome-Wide Identification and Expression Analysis of the NHX (Sodium/Hydrogen Antiporter) Gene Family in Cotton. *Front. Genet.* **2020**, *11*, 964. [[CrossRef](#)] [[PubMed](#)]
75. Paul, A.; Chatterjee, A.; Subrahmanya, S.; Shen, G.; Mishra, N. NHX Gene Family in Camellia Sinensis: In-Silico Genome-Wide Identification, Expression Profiles, and Regulatory Network Analysis. *Front. Plant Sci.* **2021**, *12*, 777884. [[CrossRef](#)] [[PubMed](#)]
76. Dong, J.; Liu, C.; Wang, Y.; Zhao, Y.; Ge, D.; Yuan, Z. Genome-Wide Identification of the NHX Gene Family in Punica Granatum L. and Their Expressional Patterns under Salt Stress. *Agronomy* **2021**, *11*, 264. [[CrossRef](#)]
77. Counillon, L.; Franchi, A.; Pouysségur, J. A Point Mutation of the Na⁺/H⁺ Exchanger Gene (NHE1) and Amplification of the Mutated Allele Confer Amiloride Resistance upon Chronic Acidosis. *Proc. Natl. Acad. Sci. USA* **1993**, *90*, 4508–4512. [[CrossRef](#)]
78. Rombolá-Caldentey, B.; Mendoza, I.; Quintero, F.J.; Pardo, J.M. Structure-Guided Identification of Critical Residues in the Vacuolar Cation/Proton Antiporter NHX1 from Arabidopsis Thaliana. *Plants* **2023**, *12*, 2778. [[CrossRef](#)] [[PubMed](#)]
79. Masrati, G.; Dwivedi, M.; Rimon, A.; Gluck-Margolin, Y.; Kessel, A.; Ashkenazy, H.; Mayrose, I.; Padan, E.; Ben-Tal, N. Broad Phylogenetic Analysis of Cation/Proton Antiporters Reveals Transport Determinants. *Nat. Commun.* **2018**, *9*, 4205. [[CrossRef](#)]
80. Zhang, Y.; Xu, J.; Li, R.; Ge, Y.; Li, Y.; Li, R. Plants' Response to Abiotic Stress: Mechanisms and Strategies. *Int. J. Mol. Sci.* **2023**, *24*, 10915. [[CrossRef](#)] [[PubMed](#)]
81. Masri, R.; Kiss, E. The Role of NAC Genes in Response to Biotic Stresses in Plants. *Physiol. Mol. Plant Pathol.* **2023**, *126*, 102034. [[CrossRef](#)]
82. Luo, X.; Yang, S.; Luo, Y.; Qiu, H.; Li, T.; Li, J.; Chen, X.; Zheng, X.; Chen, Y.; Zhang, J.; et al. Molecular Characterization and Expression Analysis of the Na⁺/H⁺ Exchanger Gene Family in *Capsicum annuum* L. *Front. Genet.* **2021**, *12*, 680457. [[CrossRef](#)]
83. Kodackattumanni, P.; Whitley, K.; Sasi, S.; Lekshmi, G.; Krishnan, S.; Al Senaani, S.; Kottackal, M.; Amiri, K.M.A. Novel Inducible Promoter DREB1G Cloned from Date Palm Exhibits High Fold Expression over AtRD29 to Drought and Salinity Stress. *Plant Cell Tiss. Organ. Cult.* **2023**, *154*, 367–380. [[CrossRef](#)]
84. Safdar, W.; Ahmed, H.; Bostan, N.; Zahra, N.B.; Sharif, H.R.; Haider, J.; Abbas, S. Comparative Analysis of Nine Different Small Heat Shock Protein Gene Promoters in *Oryza Sativa* L. Subsp. Indica. *Plant Syst. Evol.* **2016**, *302*, 1195–1206. [[CrossRef](#)]
85. Villain, P.; Mache, R.; Zhou, D.-X. The Mechanism of GT Element-Mediated Cell Type-Specific Transcriptional Control*. *J. Biol. Chem.* **1996**, *271*, 32593–32598. [[CrossRef](#)]
86. Sakai, H.; Aoyama, T.; Oka, A. Arabidopsis ARR1 and ARR2 Response Regulators Operate as Transcriptional Activators. *Plant J.* **2000**, *24*, 703–711. [[CrossRef](#)] [[PubMed](#)]
87. Li, D.; Xu, R.; Lv, D.; Zhang, C.; Yang, H.; Zhang, J.; Wen, J.; Li, C.; Tan, X. Identification of the Core Pollen-Specific Regulation in the Rice OsSUT3 Promoter. *Int. J. Mol. Sci.* **2020**, *21*, 1909. [[CrossRef](#)]
88. Longsaward, R.; Pengnoo, A.; Kongsawadworakul, P.; Viboonjun, U. A Novel Rubber Tree PR-10 Protein Involved in Host-Defense Response against the White Root Rot Fungus *Rigidoporus Microporus*. *BMC Plant Biol.* **2023**, *23*, 157. [[CrossRef](#)] [[PubMed](#)]
89. Marand, A.P.; Eveland, A.L.; Kaufmann, K.; Springer, N.M. Cis-Regulatory Elements in Plant Development, Adaptation, and Evolution. *Annu. Rev. Plant Biol.* **2023**, *74*, 111–137. [[CrossRef](#)] [[PubMed](#)]
90. Kumar, P.; Choudhary, M.; Halder, T.; Prakash, N.R.; Singh, V.; V, V.T.; Sheoran, S.; T, R.K.; Longmei, N.; Rakshit, S.; et al. Salinity Stress Tolerance and Omics Approaches: Revisiting the Progress and Achievements in Major Cereal Crops. *Heredity* **2022**, *128*, 497–518. [[CrossRef](#)]
91. Fauzia, A.N.; Nampei, M.; Jiadkong, K.; Shinta; Sreewongchai, T.; Ueda, A. Comparative Physiological and Transcriptomic Profiling Reveals the Characteristics of Tissue Tolerance Mechanisms in the Japonica Rice Landrace Under Salt Stress. *J. Plant Growth Regul.* **2024**, *43*, 3729–3742. [[CrossRef](#)]

Disclaimer/Publisher's Note: The statements, opinions and data contained in all publications are solely those of the individual author(s) and contributor(s) and not of MDPI and/or the editor(s). MDPI and/or the editor(s) disclaim responsibility for any injury to people or property resulting from any ideas, methods, instructions or products referred to in the content.